INNER FOREARC SEQUENCE ARCHITECTURE IN RESPONSE TO CLIMATIC AND TECTONIC FORCING SINCE 150 ka: HAWKE'S BAY, NEW ZEALAND.

FABIEN PAQUET, [1] JEAN-NOEL PROUST, [1] PHILIP M. BARNES, [2] and JARG R. PETTINGA[3]

[1] UMR Geosciences, CNRS Université de Rennes 1, Campus de Beaulieu, 35042 Rennes cedex, France email fabien.paquet@univ-rennes1.fr

[2]National Institute of Water & Atmospheric Research (NIWA), Private Bag 14-901, 301 Evans Bay Parade, Greta Point, Wellington, New Zealand

[3] Department of Geological Sciences, University of Canterbury, Private Bag 4800, Christchurch, New Zealand

ABSTRACT: The influence of eustasy, tectonic deformation and sediment flux as controlling parameters on basin stratigraphy and depositional sequence development are largely accepted. Eustasy is usually considered as the dominant mechanism of sequence generation, especially for Pleistocene age successions. In active subduction margin settings, the high rates of tectonic deformation are expected to have a stronger influence on basin fill architecture, while sediment flux is generally less well constrained, and therefore less frequently considered. The active Hikurangi subduction margin in New Zealand offers the opportunity to quantitatively assess the relative roles of tectonic, climatic and eustatic drivers.

We present a quantitative source-to-sink-like study of the Late Pleistocene succession from the Hawke's Bay sector of the inner forearc domain (c. 150 ka to Present). The interpretation of a grid of high-resolution marine seismic data, onland and offshore core and well descriptions, and the integration of geomorphic studies enabled identification of system tracts. In turn these comprise two sea-level-cycle depositional sequences (LPS1 and LPS2), including one complete 100 ka sequence (LPS1). Isopach maps of both sequences reveal changes in sediment distribution and preservation that reflect the relative roles of tectonic deformation and eustasy. Eustasy dominates development of

sequence architecture at relatively short time scales (i.e., < 20-30 kyrs), whereas tectonic deformation is increasingly important at longer time scales (≥100 kyrs). Four long-lasting depocenters are identified over the inner forearc domain and located in four subsiding basins (Kidnappers, Mahia, Lachlan and Motu-o-Kura basins). Significant shifts of the depocenter location in the basins are correlated with eustatic sea level changes. Estimates of sediment volumes and masses from isopach maps indicate higher mass accumulation rates during climato-eustatic extremes, which we correlated to the onland erosional response.

Sediment distribution and landscape evolution are strongly influenced by the interaction of the structural deformation and sediment flux. We present paleogeographic reconstructions for the inner forearc domain coincident with two paleoclimatic extremes (Last Glacial Maximum and Holocene Optimum). These illustrate the importance of eustatic changes, structural deformation and sediment flux on the pattern of sediment distribution, accumulation and sequence architecture.

Keywords : Sequence stratigraphy, sedimentation, forearc basin, active margin, climate, eustasy, source to sink, New Zealand.

INTRODUCTION

Eustasy, climate and tectonic deformation are key parameters that control erosion, sediment supply and transport, deposition and preservation and thus stratigraphic patterns in sedimentary basins (Jervey 1988; Posamentier et al. 1988; Blum and Törnqvist 2000). This is particularly emphasized during the Pleistocene as high amplitude climate-driven eustatic changes influence the development of depositional sequences. Classical Atlantic-type passive margin settings are characterized by extensive continental source regions with relatively subdued topography, simple shelf ramp and upper slope morphology reflecting moderate regional subsidence of the continental margin (Payton 1977), relatively low sediment supply, and eustatic sea-level changes that control the distribution and preservation of sediments (*e.g.* Vail et al. 1977). In tectonically quiet or passive settings marginal to active plate boundaries, the architecture of sedimentary successions reflect interactions between high sediment supply, eustatic and climatic changes, and moderate regional uplift and/or subsidence (Saul

et al. 1999; Lu et al. 2005; Browne and Naish 2003; Naish et al. 2005; Proust et al. 2005; Duncan et al. 2000; Gulick et al. 2005). In contrast to these settings, forearc regions of active subduction margins are characterized by high rates of active tectonics, spatially and temporally varying uplift and subsidence associated with local structural evolution, relatively short, steep gradient sediment pathways, and commonly high sedimentation rates. Fault and fold structures control uplift in catchment regions, control the structure of sedimentary basins, and create complex topography that may in turn influence the distribution of sediments and the architecture of depositional sequences in forearc domains. The combined and often inter-related influences and the respective roles of tectonic deformation, sediment flux, eustasy, and climate change on topography, accommodation space, and stratigraphic architecture, is rarely well illustrated or understood on such active margins (Okamura and Blum 1993; Christie-Blick and Driscoll 1995; Catuneanu 2006).

The upper Pleistocene stratigraphy of the Hawke's Bay region of the active Hikurangi subduction margin, New Zealand (Fig. 1), represents an ideal location to improve understanding of inner forearc sequence architecture in response to climatic and tectonic forcing and its inter-relationship with eustasy changes. The region is undergoing rapid tectonic deformation (Beanland et al. 1998; Cashman and Kelsey 1990; Barnes et al. 2002; Litchfield and Berryman 2006), and contains an excellently preserved record of erosion and sedimentation during a complete high-amplitude climatic-eustatic cycle (*i.e.*, since 150 ka – *e.g.* Lewis 1971a, 1973). Interpretation of extensive data in this region enables us to (1) characterize the marine sedimentary architecture beneath the shelf and upper trench slope basins (seismic facies and units, stratigraphic architecture, age controls); (2) evaluate terrestrial sediment responses to climate change and uplift in the inner forearc foothills and mountainous catchments; and (3) integrate these components of the forearc domain into a "source to sink" model. These results enabled us to develop two end-member sequence stratigraphic models of the paleogeographic evolution of the inner forearc, characteristic of glacial and interglacial conditions. Based on this we evaluate the sediment budget of the margin since 150 ka, and explore relationships between the marine and non-marine morphostructural evolution. We show that the Late Pleistocene evolution of the Hawke Bay forearc domain results from the interaction of both long and short-term climatic and tectonic forcing factors.

This study presents the interpretation and integration of a large dataset acquired both in the onshore and in the marine parts of the forearc domain in the Hawke's Bay region (Fig. 2). The onshore data were provided by fieldwork as part of this study, as well as published interpretations of fluvial terraces and groundwater boreholes. The marine data include an extensive grid of seismic reflection profies of variable resolution and depth of penetration (3.5 kHz, boomer, airgun multichannel (MCS)), bathymetry data and sediment cores (Appendix 1; Fig. 2).

REGIONAL SETTING OF THE HAWKE'S BAY FOREARC DOMAIN

Tectonic Evolution and Geomorphic Domains

The active Hikurangi margin of New Zealand is characterized by oblique subduction of a thickened wedge of the oceanic Pacific plate beneath the continental crust of the North Island of New Zealand (Australian Plate) (Fig.1). The present day structure of the margin is the result of polyphase tectonic evolution. Subduction started during the early Miocene about 25 Myrs ago (Ballance 1976; Pettinga 1982; Spörli and Ballance 1989; Chanier 1991; Field and Uruski 1997) and tectonic deformation has been dominated by thrust faulting, with a Late Miocene-Pliocene phase of shallow extension followed by further shortening and inversion (Chanier et al. 1992; Buret et al. 1997, Barnes et al. 2002; Barnes and Nicol 2004), and strike-slip deformation along the axial ranges since 1-2 Ma (Nicol et al. 2007 and references herein).

The active margin comprises a series of approximately parallel NE-SW-striking domains (Lewis and Pettinga, 1993) (Fig. 1D). From west to east these include:

1) A **volcanic arc** (Central Volcanic Zone) and **backarc rift** merging along strike into the subsiding Wanganui Basin;
2) Flat-topped **axial ranges** representing the frontal ridge (Fig. 3), composed of Mesozoic basement rocks that are being uplifted by dextral-reverse faults, and deeply eroded by a network of V-shaped river valleys with localized aggradational terraces (Smale et al. 1978; Beanland et al. 1998; Litchfield 2003). The emergence of the ranges occurred close to the Plio-Pleistocene boundary (Beu et al., 1981; Erdman and Kelsey, 1992), with uplift rates of 1.0-1.3 $mm.yr^{-1}$ (Beu et al., 1981; Litchfield and Berryman, 2006);

3) Rounded **foothills** consisting of uplifted and emergent Miocene to Pleistocene marine and terrestrial sediments of the formerly-wider forearc basin, deformed by thrust faults and gentle folds (Grant-Taylor 1978; Cashman et al. 1992; Beanland et al. 1998).These foothills are incised by wide U-shaped river valleys with sets of cut and fill terraces (Litchfield and Berryman 2005). Uplift rates for the last 125 ka, derived from fluvial terrace elevations (Litchfield and Berryman 2006), range from 3 $mm.yr^{-1}$ along the Ruahine range-front to <1 $mm.yr^{-1}$ further to the east;

4) An irregular, 20-30 km wide, **actively subsiding forearc basin** filled by up to 3000m of Mio-Pliocene deep marine sediments and Plio-Pleistocene shallow marine to fluvial sediments (Ballance et al. 1982; Proust and Chanier 2004), and bounded by major thrust and reverse faults (Cashman et al. 1992; Beanland et al. 1998; Barnes et al. 2002). The sedimentation rate is estimated to have reached 3.6 $mm.yr^{-1}$ during the last 18 kyr (Litchfield and Berryman 2006) on the coastal Heretaunga Plains. Except for these plains, the major part of the basin is currently submerged beneath Hawke Bay, with subsidence rates of the order of ~1.0-1.5 $mm.yr^{-1}$ (Pillans 1986; Proust and Chanier 2004; Cochran et al. 2006). The geometry of the active forearc basin is partially controlled by the distribution of major active structural ridges;

5) An **imbricated frontal wedge** up to about 160 km wide, the inner part of which comprises highly deformed pre-subduction and syn-subduction cover sequences that are partly exposed in the emergent coastal ranges (Pettinga, 1982) and along an outer shelf structural high that includes the Kidnappers and Lachlan ridges (Barnes et al., 2002, Barnes and Nicol, 2004). The outer part of the wedge consists predominantly of trench fill turbidites accreted beneath the middle and lower continental slope during the Quaternary (Lewis and Pettinga, 1993; Collot et al., 1996). The seafloor deepens very gradually across the shelf, at 0.1-0.2°, to the modern shelf edge at about 150 m water depth (Fig. 3). On the slope, where the average gradient is about 1°-3°, west-dipping thrust faults form a series of subparallel ridges and basins that are uplifting and subsiding respectively at rates of c. <0.5 $mm.yr^{-1}$ and up to 3 $mm.yr^{-1}$ (Lewis 1974; Lewis and Bennett 1985; Lewis and Pettinga 1993). The slope basins typically range in size from 5-30 km wide and 10-60 km long (Fig. 3). Infilling of the basins to various degrees

by predominantly hemipelagic sediment results in an overall ramp and flat bathymetric profile across the continental slope (Lewis 1980; Carter and Manighetti, 2006). The highest trench-slope basin off Hawke Bay is the Motu-o-Kura Trough, whick lies west of the Motu-o-Kura Ridge.

In this study we focus on the sedimentary evolution since 150 ka in region of the inner forearc between the axial ranges of the North Island and the toe of the lowstand sedimentary wedge in the Motu-o-Kura basin on the upper continental slope. It therefore corresponds to a quasi source-to-sink study as a small fraction of the eroded material may escape the domain through hyperpicnal or turbiditic flows as illustrated (1) by the presence of terrigeneous deposits in the lower slope-basins with mass accumulation rates (MAR) of c. 22.7g.cm^{-2}.kyr^{-1} (84% of the total MAR for the last 140 kyrs) calculatd from core MD98-2121(Carter and Manighetti, 2006) (see location on Fig. 3) and (2) by recent studies of the Waipaoa river catchment – sedimentary basin, North of Hawke Bay, where sediment escape has been evidenced (Orpin, 2004).

Climatic Evolution

In southern Hawke's Bay, a nearly 200 m deep borehole drilled in the Poukawa basin (Fig. 3), provides a complete and detailed record of late Pleistocene vegetation and climate change (Shulmeister et al., 2001; Carter, 2002; Okuda et al., 2002). Climatic conditions changed from warm and moist (podocarp/hardwood forest) at the last interglacial (Oxygen Isotopic Stage 5) to colder and drier (grass and shrub lands) at the last glacial maximum (LGM) and finally to warm and moist at present day (Okuda et al., 2002). The drier conditions of the LGM probably resulted from lower precipitation and enhanced wind speeds (McGlone, 2001; Shulmeister et al., 2001) associated to a El-Niño-like conditions with dominance of westerly winds. These are illustrated by the development of tussock grassland environment. Palynological studies and climate reconstructions for the Late Pleistocene indicate a mean annual temperature decline up to c. 7°C at the LGM (Newnham et al., 1999 & 2003; Shane and Sandiford, 2003; Shulmeister et al. 2001; Barrell et al., 2005; Alloway et al., 2007; Wilmshurst et al. 2007). Glacial ice conditions in North Island were limited to the highest crests

of the southern axial ranges and to highest volcanoes of the Central Volcanic Zone at the LGM (McArthur and Shepherd, 1990; Pillans et al., 1993; Brook and Brock, 2005). No evidence of glaciation has been reported in the major segments of the axial ranges, west of the Hawke Bay.

LATE PLEISTOCENE (<150ka) STRATIGRAPHIC UNITS: SOURCE TO SINK

Late Pleistocene sediments are preserved across the source-to-sink depositional profile, including fluvial deposits of foothills domain, the actively subsiding forearc basin (coastal plain and offshore shelf), and the upper slope Motu-o-Kura Trough.

Marine Seismic Units and Unconformities

On the inner shelf boomer and 3.5 KHz profiles reveal flat lying horizons that gradually dip westward as they approach the Kidnappers ridge (Figs. 4, 5). On the outer shelf to upper slope late Pleistocene prograding lowstand wedge, characterized by sigmoidal reflectors, extends to ~500 m below the shelf edge. The seismic reflections are truncated by five major unconformities (S1 to S5) that separate six seismic units (U1 to U6) (Table 1). Within these units, eleven seismic facies (Fs1 to Fs11) are recognized (Table 2). We present three key boomer profiles from inner Hawke Bay (Lines 6, 8 and 11) (Figs. 2, 5) and two 3.5 KHz profiles (AG1 and MD152) from the mid-shelf to upper slope (Figs. 2, 6, 7).

Seismic Unit 1.---U1 forms the acoustic basement to the late Pleistocene seismic units and the core of the tectonically active Kidnappers, Lachlan and Motu-o-Kura ridges (Figs. 3, 4). In the latter case, internal reflections are highly deformed with an overall 5-10° tilt to the northwest. U1 is truncated above by a sharp erosional surface S1 (Fig. 5 and Table 2B). The two-way-travel time (TWT) thickness of U1 ranges from 150 ms to over 1.3s TWT. In the inner part of Hawke Bay, U1 is comprised of two sub-units (U1a, U1b) separated by a sharp truncation surface dipping 10° to the NW (Figs. 4, 5). The lower sub-unit U1a is made up of homogenous, high frequency, parallel reflectors (seismic facies Fs1, Tables 1, 2) interpreted as a well-bedded sandstone and siltstone succession. The upper sub-unit U1b has a sheet- to wedge-shaped reflector configuration, with low continuity, wavy to

chaotic, high amplitude reflections with superimposed channel-shape diffractions that alternate with medium continuity, sub parallel, high amplitude reflections (well-bedded) in Fs2-Fs6 (Table 2; Fig. 5). The internal unconformity between U1a and U1b, observed beneath the inner shelf, correlates to the regional unconformity that separates the Pleistocene Kidnappers Group and the Pliocene Black Reef Sandstones Formation onshore at Cape Kidnappers (Proust and Chanier, 2004) (for location refer Fig. 3). The underlying U1a is correlated to the shallow marine, regressive, sandstones and siltstones of early to mid-Pliocene Flat Rock and Black Reef Formations (Harmsen, 1985). In the middle part of U1b, a thick package of chaotic reflections correlates to the 90m- thick Clifton conglomerate exposed in the coastal cliffs, equivalent to the upper part of the Kidnappers Group (Fig. 5C) Thus, the lower half of U1b correlates to the Pleistocene Kidnappers Group deposits, that are made up of over 400 m-thick conglomerates, sandstones and siltstones strata deposited in shallow marine (inner bay to upper slope offshore) and terrestrial (fluvial, braid-fan) environments (Kingma, 1971; Kamp, 1978, 1990; Proust and Chanier, 2004). The upper half of U1b corresponds to the fluvial conglomerates and sands in the lower part of the Awatoto and Tollemache onshore wells (line 11 collected close to Awatoto well, see Figs. 2, 5A, 8). Core sampling from the mid-shelf to upper slope strata by the R/V Marion-Dufresne in 2006 further corroborates these correlations in the inner bay. Two long piston cores MD06-2995 and MD06-2996, of respectively 19 m and 26.8 m, penetrated U1 over the Motu-o-Kura ridge, at approximately 500 m of water depth (Fig. 2). These sediments are made up of gas-rich, highly compacted, silty mud (Proust et al., 2006). The absence of *Bolivinita pliozea* and the presence of more than 25% of sinistral form of *Gr. truncatulinoides* in the basal part of MD06-2995 are consistent with an age younger than 0.5 Ma (B. Hayward pers. comm., in Proust et al., 2006). The absence of *Bolivinita pliozea* and the presence of dextral *T. truncatulinoides* in the basal part of MD06-2996 (B. Hayward pers. comm. in Proust et al., 2006) are consistent with an age ranging from 0.5 -0.6 Ma (Fig. 6). Three 1 to 2 m-long piston cores MD06-2998 to3000, penetrated U1 over the Kidnappers ridge in 70-90m of water depth (Fig. 2). These sediments correlate to the mid-Pleistocene Series (630-400 kyr) noted in Barnes and Nicol, 2004), and confirm the interpretation of U1 as Plio-Pleistocene in age, but also imply that the whole mid-Pleistocene to Present section is condensed below the shelf break, at circa 500 m of water depth (Figs. 4, 6).

Seismic Unit 2.---Beneath the inner shelf,U2 is a 160 ms TWT thick wedge-shape unit thinning out eastward against the Kidnappers ridge (Figs. 4, 5) and locally tilted 1-2°NW. Beneath the outer-shelf and upper slope region, U2 is more than 300 ms TWT thick, lens shaped (Fig. 9A), and locally deformed by active structures. U2 lies conformably on surface S1 with evidence of rare onlapping reflections beneath the upper slope (Fig. 9A). It is truncated above by an irregular, channeled surface (S2) dipping 1° NW in the SE and flattening to the NW (Fig. 9B).

On the shelf, U2 is made up of facies Fs2 with sub-parallel, low continuity reflections above S1 passing upward to chaotic reflections with diffractions below S2 (Fig. 5, Table 2). On the outer shelf and upper slope, U2 is comprised of three seismic facies (Fs7, Fs8, Fs9) organized in 100ms-thick (TWT) lens-shaped seismic reflection packages bounded by conformable high amplitude surfaces that are correlated with difficulty around the seismic grid (Fig. 9A). In an individual seismic package, Fs9 exhibits reflections with a regular sub-parallel configuration and good continuity that pass progressively to a sub-parallel, wavy (seismic facies Fs8) configuration in a basinward direction, while to landward a reflection free configuration (seismic facies Fs7) is evident. Towards the top of the unit, the seismic facies becomes progressively more chaotic. The stacking arrangement of seismic reflection packages exhibit an initial retrogradational followed by progradation pattern (Fig. 9A). This progradational stacking pattern appears in both the Lachlan and Motu-o-Kura basins, where lens shape packages are separated by clear downward shifts (Fig. 9A and 9B). In the Lachlan basin, the downward shift trend reveals a SW progradation of packages, along the axis of the basin.

On the inner shelf, surface S1 can be geometrically correlated from seismic profiles to (1) the large and well preserved marine terrace that topped the Kidnappers cliffs, and (2) to the first marine incursion observed in the coastal wells, by converting all data at the same scale (well, seismic and topographic cross sections - Fig. 8 and 10). In addition to geometric features (*e.g.*strike, dip), the strength of the S1-Kidnappers marine terrace correlation is supported by common features that both surfaces share (*e.g.* straight and sharp wave cut-like erosion of the tilted Kidnappers Group series – Fig. 10). The age of the marine terrace at Cape Kidnappers is deduced from (1) its height, 120 to 180 m above present day sealevel, with respect to localHolocene uplift rates (c.1 to c.2 $mm.yr^{-1}$), derived from younger Holocene marine terraces height (Hull, 1985; Hull 1987), (2) from the loess stratigraphy

(three loess layers) that overlies the terrace, which is consistent with the MIS 5 (Hull, 1985 and personnal communication), and (3) the observation that the terrace cuts almost horizontally the tilted Kidnappers Group (c. 1 to c. 0.45 Ma; Proust and Chanier, 2004). The S1 surface correlates offshore to the wave ravinement surface (WR) of the last interglacial (MIS 5e), wedging out against the Kidnappers ridge (Lewis, 1971a; Barnes et al., 2002). Seismic facies Fs2 is interpreted as an alternation of shallow marine siltstones and sandstones passing upward to stacked lenses of channelized terrestrial conglomerates interbedded with sandstone strata. This interpretation is supported by the overall coarsening upward succession of shallow marine silty sands and fluvial gravels observed in the wells (Fig. 8). This succession is organized into a set of parasequences that can be correlated to the MIS5-MIS3 sea level changes. In the outer part of the Hawke Bay seismic facies Fs7, Fs8 and Fs9 are interpreted to correspond to a series of massive to well-bedded sandstones and siltstones that pass basinward to a set of large scale bedforms interpreted as sediment waves. This last facies becomes more chaotic up section. Fs7, Fs8 and Fs9 are arranged into progradational facies tracts that are organized into a broad retrogradational and then progradational stack, with two landward stepping packages overlain by three seaward stepping packages respectively (Fig. 9A and 9B). The shallowing upward succession of shallow marine sandstone and siltstone to fluvial conglomerates, gives rise to a laterally deepening and vertically shallowing stack of sequences comprised of shore-connected, massive sandstones with channels (Fs7), well bedded marine siltstones (Fs8) passing basinward to sediment waves (Fs9).

Seismic Unit 3.---Beneath the inner shelf U3 is a thin, 10 to 20 ms thick (TWT), slightly concave up, discontinuous, sheet drape unit. Reflections onlap at the base onto S2, and are either concordant, or truncated above, along S3 (Figs. 4, 5; Table 1). S2 is an irregular truncation surface with channels that transition to a concordant surface in a seaward direction from the northern part of the Lachlan basin (Figs. 6, 7, 9B) to the offshore. S2 truncates U2 as it approaches the structurally active ridges. Nevertheless S2 is not preserved on top of the active ridges (Figs. 5, 7).

Beneath the shelf, U3 is ~50-100 ms TWT thick, and made up of random alternations of stacked, channel shaped, and minor sub-parallel reflections assigned to seismic facies Fs3. On the outer shelf to upper slope, U3 is made up of facies Fs9, Fs10, and Fs11. Fs9 exhibits sub-parallel, high continuity,

medium amplitude reflections that pass upwards to chaotic, high amplitude reflector configurations in Fs10, or in a seaward direction, to wavy, parallel and highly continuous reflections in Fs11 (Fig. 6, Table 2). The latter are characterized by long thin and faint lee-side reflections and usually short, thick and high amplitude stoss-side reflections. The stacked wavy undulations exhibit an apparent progressive landward/upslope migration (S-type sediment wave) (Fig. 6) together with a convex-upward geometry and a decreasing height and wavelength. Reflection-free configuration patches occur randomly into Fs11 on the seaward dipping side of the undulations. The seaward end of Fs11 coincides with the progressive wedging-out and condensation of its internal reflections as they approach the first slope scarp of the imbricate frontal wedge at a water depth of c.500m.

The S2 surface is an irregular truncation surface with channels incised into lenses of inferred terrestrial gravels interbedded with sands. It geometrically correlates to the maximum downward shift in base-level next to the base of the thickest gravel bed in the coastal wells (Fig. 8). It is interpreted as the last sequence boundary (SB) of the last glacial maximum (MIS 2, ~20 kyr). The overlying facies Fs3, on the shelf, is interpreted as fluvial, channel belt gravel and overbank sand deposits. It passes basinward to well-bedded marine sands and silts (Fs9, Fig.6) that give rise at the shelf edge to massive sands and channels of high amplitude chaotic configurations (Fs10). Below the shelf edge Fs10 passes to wavy reflections Fs11. Fs11 geometries are consistent with an extensive field of upslope migrating sediment waves (Lee et al., 2002). This interpretation differs from those of Lewis (1971b) and Barnes and Lewis (1991), who interpreted these undulations as the extensive Kidnappers slide mass. Our re-interpretation of the "Kidnappers slide" as a field of sediment waves is based on (1) the absence of both a major headscarp wall at the upper end and a shortening zone at the lower end, (2) the good continuity of some seismic reflectors on both sides of the supposed fault plane, and (3) the unsusual downward attenuation of deformation along fault plane-like features (*e.g.*, Lee et al., 2002)(Fig.6). A 30 m-long piston core (MD06-2997) penetrated through the whole Fs11 sediment wave package, and revealed bioturbated silty to sandy clays with organic rich layers resting over gas-rich liquefied mud. The presence of gas at the base of the core is compatible with the base of a reflection free patch seen on the 3.5 KHz profile (Fig. 6). Radiocarbon measurements on shell samples taken from two former cores, Q942 and S784 (Barnes et al., 1991), penetrating the top of U3, provide respective ages of

19,240±310 yrs to 18,060±200 yr (c. 23 ka to c. 21.5 ka in calendar years – Fig. 6). Preliminary tephra identification at the uppermost part of MD06-2996, where U3 thins out almost completely (Fig. 6), provided age estimations ranging from c.50 to c.30ka (Philip Shane, personal communication). This confirms that the upper part of U3 was deposited during the last glacial maximum between c.25 to c.21 ka (Pahnke and Sachs, 2006).

Seismic Unit 4.---U4 is a 30 ms thick (TWT) wedge-shaped unit that is only represented in inner Hawke Bay (Figs. 4, 5). It pinches out to the SE against the west flank of the Kidnappers ridge. It is slightly tilted seaward (~1°) except for local deformation along the Kidnappers Ridge (Fig. 5B). U4 reflections clearly onlap S3 and are truncated above by a sharp and planar erosion surface S4. U4 is made up of seismic facies Fs3 with sub-parallel, highly discontinuous, wavy and channel-shape reflectors.

S3 is interpreted as a transgressive surface (TS) onlapped by U4 fluvial sediments inferred to have formed during post-glacial sea-level rise. S3 is tentatively correlated to the change from fluvial gravels to fluvial sandy gravels at 35m depth in the Awatoto well (Fig. 8). The sandy gravels are bracketed by two dated samples, 10247±99yrs BP at base and 7889±114 yrs BP (radiocarbon ages) at top, that constrain the late stage of post-glacial sea level rise in the inner part of Hawke Bay (Dravid and Brown, 1997). This corresponds more or less to a rapid sea level rise from c. -30m to c. -9m according to Gibb's sea level curve (Gibb, 1986).

Seismic Unit 5.---U5 is a 25-40 ms thick (TWT), bank to lens shape, slightly concave up unit that thins out toward the coastline and drapes over the active ridges (Fig. 4). It reaches a maximum thickness across the inner shelf in Hawke Bay and immediately landward of the shelf edge, offshore Waimarama coast (Figs. 4, 6, 7). U5 internal reflections onlap onto a sharp and planar erosion surface of regional extend S4 (Figs. 5, 7). S4 extends across the entire inner bay, truncating all units adjacent to Kidnappers ridge (Fig. 5). U5 is bounded above by a concordant surface S5 that dips slightly seaward and is overlain by downlapping reflections (Fig. 6). In the inner bay, U5 is comprised of low amplitude, average continuity and frequency, sub-parallel reflections of seismic facies Fs4 (Fig. 5, Table 2). In the outer bay, U5 is made up of sub-parallel, continuous reflections of seismic facies Fs7 which drape the undulations of Fs11 below the shelf edge (Fig. 7).

The basal S4 planar erosion surface is interpreted as the wave ravinement surface (WR) that developed as the sea flooded the area during the postglacial sea level rise (c.20 to c. 7 ka BP; Gibb, 1986; Carter et al., 1986; Cochran et al., 2006, Lamarche et al., 2006). Numerous authors have previously recognized this prominent surface along the East Coast margin (Lewis, 1973a; Foster and Carter, 1997; Barnes et al., 2002). The upper surface (S5) is dipping slightly seaward and is interpreted as the maximum flooding surface (MFS) formed as the sea reached its highest elevation at the Holocene optimum ~7 ka B.P.

In the inner shelf, U5 is interpreted as a horizontal, poorly bedded silts and sands succession, probably deposited in a high to moderate energy, marine shelf environment (seismic facies Fs4). These deposits are time equivalent to the coastal and floodplain carbonaceous silty clays (Fig. 8) preserved at the back of a prominent retrogradational gravel beach on land (U4; see also Dravid and Brown, 1997). In the outer parts of Hawke Bay, U5 is comprised of Fs7 sub-parallel, continuous reflections that represent marine silts and sands. Piston cores MD06-2998 and MD06-3000 probably penetrated U5 where it thins out over the Kidnappers Ridge. It is made up of poorly sorted pebbly-muddy sands that may correspond to retrogradational shore deposits.

Seismic Unit 6.---U6 is a 10-35 ms thick (TWT), sheet drape to lens-shaped unit dipping slightly seaward (Figs. 4, 5). U6 drapes most of the shelf and upper slope and, as for U5, thickens markedly offshore from the Waimarama coast (Fig. 6). Below the shelf edge, U6 thins out rapidly and can hardly be distinguished from U5, as they show almost no internal reflections. The internal reflections downlap onto a concordant surface S5 and are either truncated, or gently top-lapped, by the seafloor above.

In the inner parts of Hawke Bay, U6 is made up of low amplitude, oblique parallel to sigmoidal reflections in dip direction, and parallel reflections in an along strike direction (facies Fs5) (Fig.5). Further offshore, U6 is comprised of sub-parallel, low continuity to reflection free (seismic facies Fs8). Below the shelf edge, this facies drapes the undulations observed in U5 and U3 forming a wavy seabed.

On the shelf, facies Fs5 is interpreted as poorly bedded, marine silt deposit prograding towards the shelf break. These moderate to low energy deposits are capped inland by coastal and floodplain

deposits (Fig. 8). On the upper slope, sediment collected in the down-lapping seismic facies Fs8, from the top of cores MD06-2997 and MD06-2998 (Fig. 6) are made up of marine bioturbated silty to sandy clays and clayey silts and sands with shell debris. Tephra and shell samples from former shallow cores in the same unit (*e.g.* Q939 and S783) provide ages ranging from 6,644 yr±98 to 1,215±78 yr B.P. (Barnes et al., 1991). U11 is interpreted as a prograding marine highstand system tract (HST) developed along the MFS since the Holocene optimum (7.2 kyr).

Terrestrial River Terraces and Cover Deposits

Flights of uplifted fluvial aggradation terraces are well preserved along the major river valleys (Tukituki, Ngaruroro, Mohaka, Wairoa) within the foothills domain of Hawke's Bay (Litchfield, 2003; Litchfield and Berryman, 2005). Aggradation deposits are comprised of sandy gravels derived from Mesozoic greywacke basement exposed in the axial ranges. The aggradation gravels are occasionally overlain by fluvial (overbank) silts and/or loess beds. Occasional tephras from the Central Volcanic Zone (see Fig.1) are intercalated and visibly preserved in the terrace deposits. The terrace cover deposits are typically ~6 m-thick but can locally reach up to ~30 m (Litchfield, 2003). Litchfield (2003) and Litchfield and Berryman (2005) correlate four major terrace fill units (T1 to T4) between catchments along Eastern North Island, using different age calibration methods, including 14C, optical simulated luminence (OSL) and tephrostratigraphy. The most extensive and best dated of these terraces are T1, T2 and T3 (Fig. 11). In addition to OSL ages of T1 (16.3±1.5 to 23.9±1.8 ka), Litchfield and Berryman (2003) have identified the Kawakawa tephra within the terrace fill deposits. Age of the Kawakawa tephra is well determined at c. 26.5 ka - Frogatt and Lowe (1990). T1 is topped by a thin loess (Loess 1) dated at between 11.2±0.8 to 13.2±0.9 Kyr using OSL and including Rerewhakaaitu tephra (c.17.7 ka). Thus, aggradation of T1 started at the end of marine oxygen isotope stage (MIS) 3 (c. 30 ka) and finished at c. 15 ka, before the end of MIS 2 (c.13 ka) (Fig. 12).

The age of T2 aggradation is constrained by the Kawakawa (c. 26.5 ka) and the Omataroa (c. 30.5 ka) tephras. T2 formed during the MIS3 cooling stage that occurred at c. 40 ka (Fig. 12). T3 cover deposits are dated from 67.6±6.8 to 75.3±5.5 kyr using OSL, and including the Rotoehu tephra. Age of the Rotoehu tephra is still subject to some debates but generally varies from c.40 to c.71±6 ka (Pullar

and Heine, 1971; Berryman, 1992, Wilson et al., 1992; Lian and Shane, 2000, Shane and Sandiford, 2003). Two distinctive loess formations top the T3 fluvial deposits. They are identified as Loess 1 (also T1 loess cover) overlying Loess 2 (39.7±2.5 kyr OSL) (Litchfield and Berryman, 2005). The aggradation of T3 terrace occurred during MIS4 (c.59 to c.72 ka), probably from ~80 to c. 60 ka (Fig. 12).

Older uplifted terrace remnants, including the Salisbury terrace (Kingma, 1958; Raub, 1985), are also locally present in the foothills domain between Ngaruroro and Tukituki catchments. A topographic section across the foothills from the Tukituki to the Ngaruroro Rivers reveals the presence of two elevated and dissected, remnant terrace surfaces (Figs. 11). The topmost is the widespread Salisbury terrace at c.550 m elevation (Fig. 11A). The second, referred to as "T4", is located immediately below the Salisbury terrace at c.400 m elevation, and is observed south of Ngaruroro River (Fig. 11B). Except for rare examples in other catchments (Litchfield and Rieser, 2005), age control on these terraces is lacking but an estimate of the stratigraphic position of these older terraces is possible. By combining old terrace elevations with younger age-dated terraces from Litchfield and Berryman (2006), it is possible to infer an age ranging from c. 120 ka to c. 100 ka (MIS5) for the T4 terrace and an age ranging from c. 150 ka to c. 130 ka (MIS6), for the Salisbury terrace (Fig. 11). The latter estimation is compatible with the youngest ages of the underlying sedimentary succession of mid-Pleistocene age (Raub, 1985; Shane et al., 1996; Paquet 2007) (Fig. 11A). These data are also consistent with the average local uplift rates of the foothills domain (c.1.5 to 2.5mm.yr^{-1}, Fig. 11C) (Litchfield and Berryman, 2006).

The phases of terrace aggradation are separated from periods of river incision. The formation of terrace cover sequences broadly correlates with late Pleistocene cool/cold periods while incision corresponds to warm stages (Figs. 12B, 13B – see Discussion).

TWO MAJOR SEDIMENTARY SEQUENCES CORRESPONDING TO THE LAST TWO CLIMATIC-EUSTATIC CYCLES (<150 KYRS)

Correlation of the sedimentary units and seismic facies to marine sediment cores, Hawke Bay #1 well, coastal borehole data, and onland exposures (Appndix 1) enabled us recognise a wide range of

sedimentary environments within the deposits across the inner forarc region (Tables 1, 2; Fig. 14). These include (1) fluvial channel and overbank (flood plain) gravels, sands and silts; (2) coastal plain and lagoonal sands and silts; (3) shoreface gravels and sands; (4) shallow marine sands and silts; and (5) upper slope silts and muds. Consideration of the geometry of the marine sedimentary units, their unconformities, facies relationships, depositional environments, and age control, and integration of the units with coeval fluvial terraces, allow us to identify two major, tens to hundreds of metres thick, late Pleistocene climato-eustatic sequences that span the entire inner forearc region from the foothills domain to the upper slope Motu-o-Kura basin (Fig. 12; see also Fig. 4). We demonstrate below that the lower sequence (Late Pleistocene 1 - LPS1) represents a complete climato-eustatically driven 100 ka-type depositional sequence corresponding to marine oxygen isotope stages (MIS) 6 to 3 (c. 150 ka to 30 ka). The upper sequence (Late Pleistocene 2 - LPS2) corresponds to MIS 2 to 1 (c. 30 ka to Present).

Late Pleistocene 1 (LPS1): MIS 6 to MIS 3 (150 to 30 ka)

Sequence LPS1 is preserved in river valleys and in several onshore-to-offshore basins (Kidnappers, Lachlan, Motu-o-Kura) bounded by tectonically active ridges (Fig. 4). The sequence rests unconformably on a deformed Plio-Pleistocene substrate (seismic unit U1) that is exposed at the seafloor along the Kidnappers, Lachlan and Motu-o-Kura ridges (Fig. 5C). On the shelf, the unconformity at the top of U1 is the sharp, planar ravinement surface S1. On the outer shelf and upper slope, S1 is an onlap surface that becomes progressively concordant in a basinward direction. The top of LPS1 is defined by an extensive surface (S2) characterized by reflector truncations and channel incisions. This surface becomes concordant beyond the shelf edge, and is interpreted as a sequence boundary.

Over the inner shelf, within the Kidnappers basin, LPS1is made up of thin basal, deepening up, transgressive marine sands overlain in turn by a shallowing upward succession of shallow marine silts and sands to floodplain and fluvial sands and gravels (seismic unit U2) (Figs. 5, 8 and 14). From mid-shelf to upper slope, within the Lachlan and the Motu-o-Kura basins, the sequence exhibits deeper

water paleoenvironments, with massive to well-bedded marine sands and silts passing basinward to a set of large-scale bedforms interpreted as sediment waves, but with retrogradational and progradation geometries that are interpreted to reflect the deepening and shallowing up trends observed on the shelf. These trends correspond respectively to lowstand, transgressive, highstand and regressive systems tracts of an individual depositional sequence (Figs. 9, 13). Towards the top of U2 in the offshore, LPS1 is characterized by a chaotic facies interpreted as channelized and remobilized sediments. The substantial volume of sediment involved is attributed to a relative sea level fall immediately predating the formation of unconformity S2.

The age of LPS1 is bracketed by: (1) the age of the condensed section at the base of the sediment waves (U1) dated at ca. 500 ka to 600 ka (Proust et al., 2006); (2) the age of the uplifted marine terrace at Cape Kidnappers (Lewis, 1971a; Hull, 1985) geometrically projected to S1 and dated at c. 120 ka; and (3), the age of the Te Rere tephra (~25 ka) sampled in the upper part of U3 in sediment cores (Barnes et al., 1991). We therefore correlate the basal ravinement surface S1 to the last interglacial sea level rise that occurred from c. 135 to 125 ka (MIS6 to MIS5). As S1 is a composite surface that evolves offshore as a sequence boundary-type surface, we infer that the base of LPS1 corresponds to the penultimate glacial sea level maximum fall c. 150 ka (c. -110m). The topmost unconformity S2 correlates to the LGM ~25 ka. Accordingly, the LPS1 sediments record the last interglacial MIS6 to MIS5 period of time, and the overall glacial sea-level fall that occurred from MIS5 to MIS2. These correlations are corroborated by two landward stepping offshore units that represent the transgressive and early highstand systems tracts of LPS1, overlain by three seaward stepping units that are related to the three main stages of the late highstand and regressive systems tracts in LPS1 (MIS5d, MIS5b and MIS4) (Figs. 9, 13).

The development of aggradational cover sequences on terraces T2, T3 and T4 are coeval with the deposition of these seaward stepping marine units of LPS1 observed beneath the outer shelf and upper slope (Fig. 7). The older Salisbury terrace is considered as the penultimate glacial maximum equivalent of the youngest terrace T1. Its offshore equivalent is inferred to be the basal lowstand deposits of LPS1 (Figs. 9, 13B). This scenario implies that the terrace strath correlates to the sequence boundary unconformity at the base of a 100 Kyr terrestrial -to-marine depositional sequence.

Late Pleistocene 2 (LPS2): MIS 2 to MIS 1 (30 ka -Present)

Sequence LPS2 provides the most accessible and best-resolved record of glacial and interglacial environments across the inner forearc region. The sequence lies on the strath of terrace T1 in river valleys, on the LGM unconformity S2 on the shelf, and on a concordant surface on the slope. On the inner shelf it is draped over both the subsiding basins and the ridges, and comprises four seismic units U3, U4, U5, and U6, respectively bounded above by surfaces S3, S4, S5 and the sea floor (Figs. 4, 5, 13). On the mid shelf and upper slope, in the Lachlan and Motu-o-Kura basins, it comprises three seismic units, U3, U5 and U6. The surface S4 merges, locally on the ridges, with the sequence boundary S2 and the transgressive ravinement S3.

On the shelf, LPS2 includes channel fill lenses of lowstand fluvial gravels and overbank silts and sands (U3) (Fig. 14). On the outer shelf, the sequence grades upward from well-bedded, transgressive marine silts and sands to prograding, shore-connected massive sands with scattered channels. Further offshore, beyond the shelf edge, on the upper slope, it is comprised of a field of upslope migrating sediment waves made up of gas-rich, bioturbated marine silt (Fig. 6). LPS2 wedges out in the Motu-o-Kura basin at c. 500 m water depth.

LPS2 includes the lowstand, transgressive, and highstand components of the present sea-level cycle. The lowstand systems tract deposits are overlain by extensive transgressive fluvial sediments (U4) deposited during the early stage of the postglacial sea level rise above the transgressive ravinement surface S3 (Figs. 13, 14). These sediments are truncated above by a widespread, planar, strongly diachronous wave ravinement surface S4, and covered by a thin veneer of coquina sands. Surface S4 is onlapped by low energy, marine silts (U5) passing in a landward direction, through a prominent gravel beach, to coastal plain silts. The transgressive fluvial sediments together with the onlapping marine silts are part of an overall transgressive systems tract. The uppermost sediment package is composed of prograding shelf to upper slope silt (U6) downlapping onto a planar maximum flooding surface dated at 7.2 ka (S5). These silts transition on land to coastal and flood plain silts and sands with a few interclated gravel lenses (Fig. 8). U6 is the presently accumulating highstand systems tract.

This sequence stratigraphic interpretation is constrained by dated horizons, including from the base to the top: (1) the presence of both Te Rere (c. 25 kyr - Froggatt and Lowe, 1990; Nairn, 2002) in the sediment below or next to S4 (Barnes et al., 1991) and (2) the radiocarbon ages of gastropod shells collected from the merged basal unconformity (S2) and marine transgressive surface (S4) dated from 18,060±200 yr to 19,240±310 yr (Barnes et al., 1991); (3) the ages of other gastropod shells preserved in the sediment that overlies the unconformity S4 (Unit 5 & 6), dated from 6,644±98 yr to 1,215±78 yr (Barnes et al., 1991); (4) the radiocarbon age of the oldest sample collected in the uppermost part of the fluvial TST of LPS2, in the coastal plain areas that surround the Kidnappers basin, dated at 10,247±99 yr B.P. (Dravid and Brown, 1997); (5) the ages of sediments located immediately below and above the maximum flooding surface S5 ranging from c. 9,500 yr B.P. to c. 5,300 yr B.P. in the present day coastal area (Gibb, 1986; Carter et al., 1986; Cochran et al., 2006; Dravid and Brown, 1997); and (6) the ages of the Waimihia and Taupo tephras in terrestrial deposits covering the marine highstand deposits in the coastal plains dated at c. 3,450 yr and c. 1,750 yr respectively (Cochran et al., 2006; Dravid and Brown, 1997). The composite sequence boundary at the base of LPS2 therefore correlates to the last glacial maximum incision (c. 30 ka – MIS2), and the transgressive/wave ravinement surface correlates to the postglacial sea level rise that occurred from c. 18 ka to c. 7.2 ka (MIS1 to MIS2) as proposed by Gibb (1986) (Figs. 8 and 13). The maximum flooding surface, within LPS2, is correlated to the end of the last sea level rise at c. 7.2 ka (and later).

The aggradational cover sediments of Terrace T1 started developing during rapid sea level fall at the end of LPS1, and continued into the early stage of sea level rise. The terrace development was therefore coeval with the deposition of the lowstand and early transgressive systems tracts in the offshore. The river incision that followed the development of T1, commenced during the later stages of sea level rise and may be continuing today during the highstand.

SPATIAL AND TEMPORAL VARIATIONS IN SEDIMENT DISTRIBUTION

We compiled isopach maps revealing the thickness of sequences LPS1 and LPS2 (Figs. 14, 15). The TWT time intervals were converted to sediment thickness using an average velocity of 1600 $m.s^{-1}$. The

maps highlight the distribution of sediments over the entire Hawke's Bay forearc domain from the foothills terrace sequences to the toe of the lowstand systems tracts at c. 500 m of water depth.

Sequence LPS1 (150 ka to 30 ka)

The older sequence is mainly preserved in four main depocentres separated by the tectonically active ridges, including the Kidnappers, Mahia, Lachlan, and Motu-o-Kura basins (Fig. 15). It is absent over the actively rising Kidnappers and Lachlan ridges, and wedges out onto the western flank of the Motu-o-Kura ridge. The total volume of sediment preserved in LPS1 is of the order of 340 ± 50 km^3.

The Kidnappers depocentre is a broad asymmetric NE trending syncline with a steep western flank along the Napier fault, and a lower-angle eastern flank along the Kidnappers ridge. The sediment thickness reaches 160 m beneath the Heretaunga plains (present-day restricted coastal plains), decreasing rapidly southward and more progressively in a northward direction. The northern part connects to the circular-shape Mahia depocentre where sediment thickness reaches c. 150 m. The Mahia depocentre connects to the Lachlan depocentre by a c. 100 m-deep depression corresponding to the Lachlan basin syncline. The Lachlan depocentre is located in the southern part of the Lachlan basin, and sediment thickness reaches c. 150 m directly west of the Lachlan Bank. The Lachlan depocentre connects along the shelf edge to the Motu-o-Kura depocentre where sediment bodies drape the outer shelf and upper slope (Fig. 15). The maximum sediment thickness reaches c. 300 m between the shelf edge and the Waimarama coast, where active thrust faults disrupt the sediment fill. LPS1 deposits are also present in the foothills domain as terrace (T2, T3, T4 and Salisbury) cover beds up to c. 10 m thick.

Sequence LPS2 (30 ka to present)

The sequence LPS2 is widely preserved over the inner forearc region (Fig. 16). It thins out, and is locally absent, over the major active structural ridges, and it wedges out progressively with depth below the shelf edge. In the Kidnappers basin, more than half of the sequence is made up of fluvial transgressive deposits, overlain by shallow marine TST and HST. In the Motu-o-Kura basin depocentre the sequence is comprised of marine HST and TST that forms a thick wedge. The total

volume of sediment preserved in LPS2 is of the order of 140 ± 20 km^3. We estimate that the LST component corresponds to approximately one third of the total volume (c. 55 ± 8 km^3). This component includes onshore the 10 m-thick aggradational cover beds of terrace T1 in the foothills domain, estimated from fieldwork and former studies (*e.g.* Litchfield, 2003) and c.30 meter-thick gravel deposits in the restricted coastal plains, estimated from average quality onshore seimic data (not presented here) tie to Awatoto, Tollemache Orchard and other wells in the Heretaunga Plains (Dravid and Brown, 1997; this study). The major part of the LST component is primarily distributed offshore into three main depocentres, including the Kidnappers basin (offshore extension of the coastal Heretaunga Plains), the southern part of the Lachlan basin, and the Motu-o-Kura basin. In the Kidnappers basin LST sediment thickness reaches up to c. 30 m and is deposited in a broad syncline of similar shape as LPS1. These sediments thin out to the north and are minor in Mahia basin. In the contiguous Lachlan and Motu-o-Kura basins the LST sediment thickness reaches a maximum of c. 30 m below the shelf edge (Fig. 16).

The TST/HST component of LPS2 is distributed widely in Hawke Bay, as well as the coastal parts of the Heretaunga plain. We estimate that its volume corresponds to about two thirds of the total volume of LPS2 (i.e., c. 85 ± 12 km^3). Although this component thins slightly over some of the thrust ridges, its thickness is relatively less influenced by the active structures and thus its preservation is more widespread than for LPS1 or the LST component of LPS2. The TST/HST component reaches c. 60 m thickness in the Kidnappers basin, beneath the coastal Heretaunga plains (Awatoto and Tollemache Orchard wells, Fig. 8), and it thins rapidly offshore. The Mahia and Lachlan basin depocentres are is located above their LPS1 equivalents, with a sediment thickness of about 30 m. The Motu-o-Kura TST/HST depocentre is located primarily between the Waimarama coast and the shelf edge (white dashed line on Fig. 16), on the hanging wall of active thrust faults. These sediments thin dramatically off the shelf, pinching out against the Motu-o-Kura Ridge, and they are not present upstream in the foothills domain where river incision is dominating over this period of time.

RECONSTRUCTION OF THE LATE PLEISTOCENE FOREARC LANDSCAPE

We present two Late Pleistocene paleogeographic reconstructions, including: (i). a cold, dry period during a low eustatic sea level (-120 m) at the Last Glacial Maximum (~20 ka) corresponding to the LPS2 lowstand systems tracts (Fig. 17A), and (ii). a warm, moist period at a high eustatic sea level comparable to the present mean sea level (~0 m) at the Holocene optimum (~7.2 ka) corresponding to the LPS2 late transgressive to early highstand systems tracts (Fig. 17B). These reconstructions are derived from the distribution of sediments and facies presented in this study, as well as the compilation of data available in the literature (refer Fig. 17). The maps reveal how sediment dispersal is controlled by: (1) a long depositional profile with fluvial deposition from the axial range front (~300 m elevation) to the outer shelf from where it transitions to marine deposition to the toe of the Lowstand wedge (c. -500 m) during the Last Glacial Maximum; and (2) a shorter depositional profile with the beginning of long-term fluvial deposition restricted to the coastal floodplain (< 20 m) and marine deposition concentrated on the shelf (above -150 m).

The reconstruction of the depositional environments at the LGM (Fig. 17A) illustrates that fluvial gravels and overbank sands and silts were widespread in Hawke's Bay. The major rivers in southern Hawke's Bay (*e.g.* Ngaruroro, Tukituki) flowed through the Kidnappers basin before joining the northern Hawke's Bay rivers (e.g. Mohaka, Wairoa) in the Mahia basin, and turning SE into the Lachlan basin. The gravels and coarse sands occupied most of the main valleys on land and tapered in the narrow connection between the uplifted Kidnappers and Lachlan Ridges (Fig. 17A). This coarse-grained alluvial domain transitions to a contracted coastal plain, characterized by a high gradient shoreface. Such configuration is in accordance with the increase of southerly winds during LGM. This shoreface is comprised of a shore-connected, massive sand wedge with scattered channels that may correspond either to a delta front sediment wedge or an estuarine sub-tidal mouth-bar complex. This interpretation is consistent with tidal amplification induced by the narrowing between the two ridges during low sea level. With essentially no submerged continental shelf, the shoreface sands and silts rapidly transition, across an abrupt break in slope (Figs. 6, 17A), to a field of fine-grained upslope migrating sediment waves on the upper slope. Formation of the sediment wave field in the Motu-o-Kura Basin may result from (1) the large amount of LGM terrigeneous supply together with the relocation of the river outlets at the southern end of the Lachlan Basin, and (2) from the increase of the

northward flowingproto-Wairarapa Coastal Current due to a strong inflow of Sub-Antarctic Water current (*e.g*; Carter et al., 1998; Chiswell, 2000, Carter and Manighetti, 2006).

The reconstruction of the depositional environments at the Holocene Optimum provide a generalized view of marine sedimentation in Hawke Bay (Fig. 17B). It is in agreement with the present day sedimentation in Hawke Bay (Pantin, 1966) except for coastal plains where potential analogies with Holocene are less concievable. Low energy, shallow marine silts and muds cover much of Hawke Bay. It is in adequation with the seafloor On land, sedimentation is reduced except in structural depressions such as the Poukawa basin (Shulmeister et al., 2001), dominated by a lacustrine depositional environment. Sheltered embayments preserve some coarse-grained alluvial gravels at the outlet of the major rivers (e.g. Tukituki, Ngaruroro, Wairoa) and fine grained silts and clays associated with lagoonal environments (e.g. Heretaunga plains). Deposition of marine sediments is locally condensed or absent within Hawke Bay and over structural ridges, including the Kidnappers ridge in the central part of the bay and to the west of the Kidnappers Ridge.

LATE PLEISTOCENE SEDIMENT BUDGET

The mass accumulation rates of late Pleistocene sediments deposited in the inner forearc was evaluated by using volume estimations from the isopach maps (Figs. 15, 16) and mean porosity values estimated from various porosity curves and varying from 45% to 60% (*e.g.* Allen and Allen, 2005). Error estimates have been determined by evaluating the maximum and minimum values of each parameter that are used in the sediment budget calculation (*i.e*. Velocity, surface, volume, porosity, sequence duration). Errors on mass accumulation rates vary from 26% to 39% so values have to be understood with care. Nevertheless we believe that general trends are consistent.

The mass accumulation rates over the Hawke's Bay inner forearc domain range from 3.95±1.15 Mt/yr (Error: ±29%) in LPS1 to 5.67±1.97 Mt/yr (±34%) in LPS2. In the latter, LST and the combined TST-early HST accumulation rates reach 5.56±2.18 MT/yr (±39%) and 5.75±1.80 MT/yr (±31%) respectively.The late highstand sediments are interpreted to record a lower accumulation rate than the LST and TST -early HST. High mass accumulation rates on the shelf during the LGM (LPS2 - LST)

are attributed to an increase in erosion onland. This increase was also noted by McGlone et al., (1984), Newnham et al. (2003), and Harper and Collen (2002) and attributed to the replacement of protective vegetation cover (Notofagus – Podocarp forests) by unprotective shrubland and grassland over the ranges (McLea, 1990; Newnham and Lowe, 2000; McGlone, 2001, 2002). The higher accumulation rate for TST-early HST may be the result of the postglacial commencement of river incision in the foothills (Litchfield and Berryman, 2005) and the recycling of LST shelf deposits. These results are in agreement with studies of mass accumulation rates in a deeper slope basin, offshore Hawke Bay, where the terrigeneous componant doubles during glacial periods (Carter et al., 2001; Carter et al., 2006). Despite the higher LPS2 mass accumulation rates, and considering the potential errors, it appears that the mass accumulation rates are broadly constant over the late Pleistocene with an average value of 4.23±1.09 Mt/yr (±26%). This value is one third of the current suspended sediment yield estimations of 12 Mt/yr for the Hawke Bay rivers (c.11 Mt/yr) and one third of the Wairarapa Coast (c.1 Mt/yr) (Hicks and Shankar, 2003). This difference can be explained by (1) the occurrence of shelf sedimentation outside of our study area, and possible escape or loss of mud from the shelf to the deeper slope basins (also not investigated as part of this study) during either storm related and/or seismically induced submarine mass wasting, and/or (2) the increase of recent sediment supply due to the anthropogenic influence, with post-settlement (century-scale) deforestation and related erosion described by Marutani et al. (1999) and Gomez et al. (2001). The first hypothesis concerning dispersal and escape of sediment from the study area is documented by the occurrence of terrigeneous deposits in the lower slope basins offshore Hawke Bay (core MD97-2121; Carter et al., 2002; Carter and Manighetti, 2006) and by recent studies of the Hikurangi margin (Orpin, 2004). The second hypothesis has been already proposed for the Poverty Bay shelf north of our study area, where mass accumulation on the shelf during Holocene represents only ~10% of the current river sediment supply (Foster and Carter, 1997; Orpin et al., 2006). These values are consistant

DISCUSSION

Implications for Sequence Stratigraphic Models in Active Subduction Margins

In contrast to classical Atlantic-type passive margin settings with extensive but relatively subdued continental source regions, uplift of the inner Hawkes Bay forearc (axial ranges and foothills) at rates of 1-3 mm yr^{-1} (Litchfield and Berryman 2006) creates substantial youthful topography, steep gradients, and promotes erosion with fluvial systems delivering voluminous amount of coarse-grained clastic sediment to basin depocentres. The distribution of the sediment across the inner forearc region, between sediment source and "sink", clearly reflects complex interactions between eustasy, climate change, rapid tectonic deformation, volcanism and variations in sediment flux. Our results provide insights into the relative roles of the principal drivers (eustasy, climate, tectonic deformation) that control stratigraphic architecture in sedimentary basins, which are typically not easy to decipher on active margins (e.g., Christie-Blick and Driscoll 1995).

During late Pleistocene high-amplitude climato-eustatic cycles the mean rates of sea-level fall and rise reached -4 $mm.yr^{-1}$ and +11 $mm.yr^{-1}$ over c. 5-10 ka periods, respectively, (Imbrie et al. 1984; Pillans et al. 1998; Waelbroeck et al. 2002). In contrast the rates of vertical tectonic deformation associated with active structures (ridges and basins) in Hawke's Bay range from about -2 to +4 mm.yr-1 (Berryman 1993; Barnes et al. 2002; Cochran et al. 2006). The difference between these rates implies that global glacial-interglacial climate cycles and eustatic change is a first order driver of sequence architecture on the convergent margin during late Pleistocene. Whilst tectonic deformation appears to be a second order driver, the strength of the tectonic signature on basin development is dependant on the duration of the depositional sequence.

Over sufficiently long periods of time the growth of structural ridges can be sufficient to create uplift and subsidence leading to syn-tectonic growth sequences, with structural ridges forming localized barriers to sediment transport. This is revealed by the isopach map of sequence LPS1 (Fig. 15), which at 100 kyr duration, is sufficiently long for a tectonic signature to be clearly evident in the basin geometry. The active deformation across the forearc controls the structure, location and geometry of the sedimentary depocentres, as well as the pathways available for drainage and sediment dispersal. Although the total width of the inner forearc between source (the crest of the axial ranges) and "sink" (the toe of the lowstand wedge) is narrow (c. 125 km) relative to many passive margins, the sediment dispersal pathway is a circuitous route along corridors of relative subsidence located between

discontinuous, rising, thrust-faulted ridges associated with growing folds. In sequence LPS1, the effect of sea level variation on the sediment distribution is thus, relatively attenuated, compared to the influence of persistently high rates of tectonic deformation. In addition, the influence of active tectonics is also evident by the large amount of terrigenous sediment supply compared to passive margins (Milliman and Syvitski, 1992).

Over the relatively shorter period of time represented by sequence LPS2 (30 ka, and < 20 ka for the marine component on the shelf), it is clear that sediment distribution (Fig. 15) is strongly controlled by the magnitude and rate of the last sea level rise. Transgressive and highstand marine sediments in this sequence are preserved as drape over major structures including the Kidnappers Ridge and the Waimarama thrust faults on the offshore, southern shelf. The distribution of the sequence stratigraphic systems tracts reflects largely the marine transgression, and the associated changes in regional oceanic conditions. Whilst tectonic effects are evident as growth signatures in the post-glacial sequence (e.g., Lewis 1971; Barnes et al. 2002; Barnes and Nicol 2004), they mainly felt close to the shoreline, where local coseismic uplift events can have a dramatic impact on the coastal environment (e.g., Hull 1986; Berryman 1993b). At millennial and centennial timescales, catastrophic events such as large volcanic eruptions, major earthquake-generated landslides and cyclons enhance erosion and may control the sediment delivery.

Terraces aggradation deposits in the eastern foothills of the axial ranges are synchronous with cooling periods associated with sea level falls on the shelf and upper slope. Incision by rivers occurs during warm periods and sea level rises and/or stillstand/highstand. These temporal relationships differ from the traditional models that describe maximum river incision during maximum rate of sea level fall and river aggradation during sea level rise (Van Wagoner et al., 1988; Posamentier et al. 1988; Posamentier and Vail 1988; Strong and Paola 2006). However, alternative models may explain the differences in timing of river incision and aggradation observed in our study area. Such models involve either: (1) climate; or (2) both shelf morphology and sea level change as the predominant control parameters.

The first model, developed by Litchfield and Berryman (2005) for the eastern North Island rivers, proposes that climate controls sediment supply and stream power (water flux) through time and

therefore aggradation and incision in rivers. Thus, aggradation occurred during cool to cold stages as a result of: (1) increasing sediment supply to the rivers, due to enhanced erosion and slope instability within the cold and deforested axial ranges (Froggatt and Rogers, 1990; McGlone, 2001, 2002; Newnham et al., 2003; Shulmeister et al., 2004); and (2) a decrease of stream power due to dryer conditions (Shulmeister et al. 2001; Newnham et al. 2003). Incision occurs during warm and moist periods (e.g. MIS1), to compensate the effects of both aggradation and tectonic uplift, as: (1) forests regenerate in the axial ranges and prevent dramatic erosion; and (2) stream power increases along with increasing rainfall rates.

A second alternative model is based on the impact of the shelf morphology on the stream equilibrium profile during a sea level fall (Dalrymple et al. 1998). It proposes that the lengthening of river profiles on a broad and low-gradient shelf during sea level fall and lowstand conditions implies an elevation of the stream equilibrium profile above the river profile. Such a change corresponds to the creation of accommodation space along the river and favors regressive alluvial aggradation. Several examples and variations of this model are presented in the literature (Posamentier et al. 1992; Miall 1991; Shumm 1993; Dalrymple et al. 1998; Woolfe et al. 1998; Browne and Naish 2003).

The paleogeographic reconstruction of the LGM environment (Fig. 16A) including, rivers and sediment pathways at the end of the late Pleistocene regression, show that rivers flowed within the Kidnappers basins on a low-gradient emergent shelf, before turning SE to the northern Lachlan basin where they finally reached the LGM shoreline (c.-120 m). The initiation of erosional retreat was limited because the LGM shoreline did not pass beyond the shelf edge (c.-150 m) and preexisting canyons are absent on the shelf (Talling 1998). These conditions, with rivers flowing around the Kidnappers ridge, prevailed for most of the late Pleistocene eustatic sea level fall. This particular river course implies a significant lengthening of the river profiles. At the LGM, the courses of rivers were ~110 km longer than exist today in southern Hawke's Bay, and ~80 km longer in northern Hawke's Bay. The Tukituki, Ngaruroro, Mohaka and Wairoa rivers were respectively 250 km, 280 km, 250 km and 220 km long at LGM whereas present day profiles are respectively 140 km, 170 km, 170 km, and 140 km. Such lengthening of river profiles is consistent with the creation of sub-aerial accommodation space, as proposed by Dalrymple et al. (1998) and illustrated by Browne and Naish (2003) for the

South Island Canterbury plains and shelf. Thus, fluvial aggradation could have occurred in response to the lengthening of river valleys and the associated creation of sub-aerial accommodation space during eustatic sea level fall. River incision occurred when sea level stopped falling and local uplift in the foothills again became the prevalent factor influencing river behavior. Tectonic deformation and sea level changes acted together as controlling parameters on fluvial aggradation and incision and the timing of their shifts. Nevertheless, the role of climate as a controlling parameter on sediment supply and water flux provided to the system cannot be discounted. We believe that the interplay of both models is required to explain the evolution of the fluvial network during the late Pleistocene.

6- CONCLUSIONS

1. A detailed source-to-sink, stratigraphic study of late Pleistocene (< 150 ka) depositional sequences in the Hawke's Bay region of New Zealand provides constraints for deciphering the principal drivers of sequence architecture in the forearc region of a mid-latitude, temperate climate, active subduction margins. Sedimentary units and uncomformities were interpreted as system tracts and constitutive of two sea-level-cycle depositional sequences (LPS1 and LPS2), including one complete 100-kyrsequence (LPS1).
2. Isopach mapping of both sequences reveals that eustasy and its changes dominate the development of sequence architecture and sediment distribution (depocentre location) particularly at relatively short time scales (i.e., < 20-30 kyrs), whereas tectonic deformation plays an increasingly important role at longer time scales of 100 kyrs or more. Four long-lasting depocenters are identified over the forearc domain and located into four tectonically controlled subsiding basins (Kidnappers, Mahia, Lachlan and Motu-o-Kura basins).
3. We confirm observations by other workers in this region that in the foothills, fluvial terrace aggradation occurred during phases of rapid sea level fall (terraces T1, T2, T3, T4, Salisbury) and climate cooling whereas river incision occurred during sea level rise and climate warming. The terraces are here correlated with the specific marine components of their respective climatic cycles. The sediment partitioning differs from classical models that predict incision during falling stages and aggradation during rising stages. We consider that lengthening and

shortening of river profiles during rapid sea level changes modifies the accommodation space, whilst climatically induced changes in erosion rate and uplift tune the sediment supply. These processes are jointly responsible for the behaviour of the major rivers on this subduction margin.

4. Estimations of mass accumulation rates reveal higher rates during climato-eustatic extremes and abrupt transitions as for the LST, TST-early HST (LPS2) period. We correlate this with the onland response to climatic and eustatic extreme changes at LGM and Holocene optimum and related transition. Estimated late Pleistocene mass accumulation rates are half of the present day estimations of the Hawke's Bay sediment yield. This can be attributed to sediment exportation out of the studied area and/or from a recent increase of sediment supply due to anthropogenic deforestation.

5. Facies distribution within LPS1 and LPS2 along two key sections and hypothetical reconstructions of two late Pleistocene environmental extremes, corresponding to glacial and interglacial conditions, provide a detailed model of a 100 ka-type depositional sequence for the Hawke's Bay forearc domain. Postglacial rising sea level tends to restrict sedimentation on the shelf (from c. 0 m to c. -150 m) whereas glacial falling sea level tends to lengthen the depositional profile from the onshore range front (c. 300 m) to the toe of the low stand wedge (c. -500 m).

ACKNOWLEDGMENTS

This study was funded by the CNRS-INSU, CNRS Research Department n°6118 – 'Géosciences Rennes', the University of Rennes 1, the New Zealand Foundation for Research Science and Technology (Research contract CO1X0203), the Active Tectonics and Earthquake Hazards Research Programme at the University of Canterbury, and the French Ministry of Foreign Affairs. We thank the officers and technical crew on NIWA *Tangaroa* voyages, and the IPEV and Marion-Dufresne II crew for assistance with acquisition of Calypso long piston-cores. The seismic data collected by NIWA was processed by Mike Stevens with assistance from Geoffroy Lamarche. Miles Dunkin and Andrew Goh assisted with GIS applications. Alan Orpin assisted with derivation of the mass accumulation rates. This research project was undertaken under a co-tutelle agreement between Université de Rennes 1 and University of Canterbury. Nicola Litchfield assisted on the field by introducing the fluvial terrace sequence and by discussing their potential origin. Alan Hull provides additional information on the late Pleistocene marine terrace. We finally thank Craig Fulthorpe, Lionel Carter and an anonymous for their constructive reviews of this paper.

REFERENCES

Alloway BV, Lowe DJ, Barrell DJA, Newnham RM, Almond PC, Augustinus PC, Bertler NAN, Carter L, Litchfield NJ, McGlone MS, Shulmeister J, Vandergoes MJ, Williams PW, NZ-INTIMATE members. 2007. Towards a climate event stratigraphy for New Zealand over the past 30 000 years (NZ-INTIMATE project). *Journal of Quaternary Science***22**: 9-35.

Allen PA, Allen JR. 2005. Basin analysis: principles and applications. Oxford Blackwell Publishing – ISBN 9780632052073: 560pp.

Ballance PF. 1976. Evolution of the upper Cenozoic magmatic arc and plate boundary in northern *New Zealand. Earth and planetary science letters***28**: 356-370.

Ballance PF, Pettinga JR, Webb C. 1982.A model of the Cenozoic evolution of the northern New Zealand and adjacent areas of the southwest Pacific.*Tectonophysics***87**: 37–48.

Barnes PM, Lewis KB. 1991. Sheet and rotational failures on a convergent margin: the Kidnappers Slide, New Zealand. *Sedimentology***38**: 205-22 1.

Barnes PM, Cheung KC, Smits AP, Almagor G, Read SAL, Barker PR, Froggatt P. 1991: Geotechnical analysis of the Kidnappers Slide, upper continental slope, New Zealand. *Marine geotechnology* **10**:159-188.

Barnes PM, Mercier de Lépinay B. 1997. Rates and mechanics of rapid frontal accretion along the very obliquely convergent southern Hikurangi margin, New Zealand. *Journal Geophysical Research***102**: 24 931–24 952.

Barnes PM, Nicol A. 2004. Formation of an active thrust triangle zone associated with structural inversion in subducting setting, eastern New Zealand. *Tectonics***23**(1): TC1015.

Barnes PM, Nicol A, Harrison T. 2002. Late Cenozoic evolution and earthquake potential of an active listric thrust complex above the Hikurangi subduction zone, New Zealand. *Geological Society of America Bulletin***114**: 1379–1405.

Barrell DJA, Alloway BV, Shulmeister J, Newnham RM (eds). 2005. Towards a climate event stratigraphy for New Zealand over the past 30,000 years. *GNS Science Report* SR **2005/07**: 12 pp.

Beanland, S., 1995, The North Island Dextral Fault Belt, Hikurangi subduction margin, New Zealand [PhD dissert.]: Victoria University of Wellington, Wellington, New Zealand, 341 p.

Beanland S, Melhuish A, Nicol A, Ravens J. 1998. Structure and deformation history of the inner forearc region, Hikurangi subduction margin, New Zealand.*New Zealand Journal of Geology and Geophysics* **41**: 325–342.

Berryman K. 1992. A stratigraphic age of Rotoehu Ash and late Pleistocene climate interpretation based on marine terrace chronology, Mahia Peninsula, North Island, New Zealand. *New Zealand Journal of Geology and Geophysics* **35**: 1-7.

Berryman K. 1993. Distribution, age, and deformation of Late Pleistocene marine terraces at Mahia Peninsula, Hikurangi Subduction Margin, New Zealand, *Tectonics***12**: 1365– 1379.

Beu AG, Browne GH, Grant-Taylor TL. 1981: New *Chlamys delicatula* localities in the central North Island and uplift of the Ruahine Range. *New Zealand Journal of Geology and Geophysics* **24**: 127-132.

Blum MD, Törnquist TE. 2000. Fluvial responses to climate and sea-level change: a review and look forward. *Sedimentology***47**: 2–48.

Brook MS, Brock BW. 2005. Valley morphology and glaciation in the Tararua Range, southern North Island, New Zealand. *New Zealand Journal of Geology and Geophysics* **48**: 717-724.

Browne GH, Naish TR, 2003. Facies development and sequence architecture of a late Quaternary fluvial-marine transition, Canterbury Plains and shelf, New Zealand: implications for forced regressive deposits. *Sedimentary Geology***158**: 57–86.

Buret Ch, Chanier F, Ferrière J, Proust JN. 1997. Individualization of a forearc basin during the active margin evolution: Hikurangi subduction margin, New Zealand. *Comptes Rendus Académie Sciences Paris***325**: 615–621.

Carter JA. 2002. Phytolith analysis and paleoenvironmental reconstruction from Lake Poukawa core, Hawke's Bay, New Zealand. *Global and Planetary Change***33**: 257– 267.

Carter L. 1974. Sedimentation in Hawke Bay off Hastings.*NZOI Oceanographic Summary* **3**: 8 pp.

Carter L, 2001. Currents of change: the ocean flow in a changing world. *Water and Atmosphere***9**: 15-17 http://www.niwa.co.nz/pubs/wa/09-4/

Carter L, Manighetti B, Elliot M, Trustrum N, Gomez B. 2002: Source, sea level and circulation effects on the sediment flux to the deep ocean over the past 15 ka off eastern New Zealand. *Global Planetary Change* 33: 339-355.

Carter, L. and Manighetti, B. 2006. Glacial/interglacial control of terrigenous and biogenic fluxes in the deep ocean; off a high input, collisional margin: A 139 kyr-record from New Zealand. *Marine Geology* 226: 307-322.

Carter L, Garlick RD, Sutton P, Chiswell S, Oien NA, Stanton BR. 1998. Ocean Circulation New Zealand. *NIWA Chart Miscellaneous Series* **76**.

Carter RM, Carter L, Johnson DP. 1986. Submergent shoreline int the SW Pacific: evidence for an episodic post-glacial transgression. *Sedimentology* 33: 629-649.

Carter RM, McCave IN, Richter C, Carter L, et al. 1999. Southwest Pacific Gateways, Sites 1119-1125.*Proceedings of Ocean Drilling Program, Initial Reports* **181**:1-112.

Cashman SM, Kelsey HM. 1990. Forearc uplift and extension, southern Hawke's Bay, New Zealand: Mid-Pleistocene to present. *Tectonics* **9**:23-44.

Cashman SM, Kelsey HM, Erdman CF, Cutten HNC, Berryman KB. 1992. A structural transect and analysis of strain partitioning across the forearc of the Hikurangi subduction zone, southern Hawke's Bay, North Island, New Zealand. *Tectonics* **11**: 242-257.

Catuneanu O. 2006. *Principles of sequence stratigraphy*. Elsevier Science: Amsterdam; 386.

Chanier F. 1991. *Le Prisme d'accrétion Hikurangi: un témoin de l'évolution géodynamique d'une marge active péripacifique (Nouvelle-Zélande)*. Thèse de Doctorat de l'Université des Sciences et Techniques de Lille – Flandres-Artois.

Chanier F, Ferrière J, Angelier J. 1992. Extension et érosion tectonique dans un prisme d'accrétion: l'exemple du prisme Hikurangi (Nouvelle Zélande). *Compte Rendus de l'Académie des Sciences Paris***315**: série II, 741–747.

Chiswell SM. 2000. The Wairarapa Coastal Current, New Zealand. *New Zealand Marine & Freshwater Research* 34, 303-315.

Christie-Blick N, Driscoll NW. 1995. Sequence stratigraphy. *Annual Review of Earth and Planetary Sciences* **23**: 451-478.

Cochran U, Zachariasen J, Mildenhall D, Hayward B, Southall K, Hollis C, Barker P, Wallace L, Alloway B, Wilson K. 2006. Paleoecological insights into subduction zone earthquake occurrence, eastern North Island, New Zealand. *GSA Bulletin*, **118**: 1051-1074.

Collot J-Y, Delteil J, Lewis KB, Davy B, Lamarche G, Audru J-C, Barnes P, Chanier F, Chaumillon E, Lallemand S, de Lépinay BMD, Orpin AR, Pelletier B, Sosson M, Toussaint B, Uruski C. 1996. From oblique subduction to intra-continental transpression: structures of the southern Kermadec-

Hikurangi margin from multibeam bathymetry, side-scan sonar and seismic reflection. *Marine Geophysical Researches***18**: 357–381.

Conquest Exploration Co. 1988. Hawkes Bay shallow seismic and bottom sampling 38322 New Zealand. *New Zealand unpublished openfile petroleum report***1471**. Ministry of Economic Development, Wellington.

Dalrymple M, Prosser J Williams B. 1998. A dynamic systems approach to the regional controls on deposition and architecture of alluvial sequences, illustrated in the statfjord formation (United Kingdom, northern North Sea).In Shanley KW, McCabe PJ, Relative Role of Eustasy, Climate, and Tectonism in Continental Rocks. *Special Publication***59**,Society Economic Paleontologists Mineralogists: Tulsa, OK; 65-81.

Dravid PN, Brown LJ. 1997. *Heretaunga Plains—Groundwater study, Vol. I & II*. Napier, New Zealand. Hawke's Bay Regional Council: 254 pp.

Duncan CS, Goff JA, Austin JA Jr, Fulthorpe CS. 2000. Tracking the last sea level cycle: Seafloor morphology and shallow stratigraphy of the latest Quaternary New Jersey middle continental shelf, *Marine Geology***170**: 395-421.

Erdman CF, Kelsey HM. 1992. Pliocene and Pleistocene stratigraphy and tectonics, Ohara Depression and Wakarara Range, North Island, New Zealand. *New Zealand Journal of Geology and Geophysics* **35**: 177-192.

Field BD, Uruski CI and others. 1997. Cretaceous-Cenozoic geology and petroleum systems of the East Coast region, New Zealand. *Institute of Geological & Nuclear Sciences Monograph* **19**. Institute of Geological & Nuclear Sciences Ltd, Lower Hutt, New Zealand: 301pp.

Foster G, Carter L. 1997. Mud sedimentation on the continental shelf at an accretionary margin—Poverty Bay, New Zealand. *New Zealand Journal of Geology and Geophysics* **40**, 157–173.

Francis RICC. 1985. An alternative water circulation pattern for Hawke Bay, New Zealand. *New Zealand Journal of Marine and Freshwater Research* **19**:399-404.

Froggatt PC, Lowe DJ. 1990. A review of late Quaternary silicic and some other tephra formations from New Zealand: their stratigraphy, nomenclature, distribution, volume, and age. *New Zealand Journal of Geology and Geophysics***33**: 89–109.

Froggatt PC, Rogers GM. 1990. Tephrostratigraphy of high altitude peat bogs along the axial ranges, North Island, New Zealand. *New Zealand Journal of Geology and Geophysics* **33**: 111–125.

Gibb JG. 1986. A New Zealand regional Holocene eustatic sea-level curve and its application for determination of vertical tectonic movements. In Reilly, W.I., and Harford, B.E., eds., Recent crustal movements of the Pacific region: Wellington, *Bulletin of Royal Society of New Zealand***24**: 377–395.

Gomez B, Filipelli G, Carter L, Trustrum N. 2001. *Recent sedimentation on an actively subsiding shelf: Hikurangi subduction margin, North Island, New Zealand*. In: MARGINS Chapman Conference, Puerto Rico, June 2001.

Grant-Taylor TL. 1978. The geology and structure of the Ruataniwha Plains. *In:* Speden, I. *ed.* Geology and erosion in the Ruahine Range. *New Zealand Geological Survey report* **G20**:31-51.

Gulick SPS, Goff JA, Austin JA Jr., Alexander CR Jr., Nordfjord S, Fulthorpe CS. 2005. Basal inflection-controlled shelf-edge wedges off New Jersey track sea-level fall. *Geology***33**: 429-432.

Harmsen FJ. 1985. Lithostratigraphy of Pliocene strata, central and southern Hawke's Bay, New Zealand. *New ZealandJournal of Geology and Geophysics* **28**: 413 -433.

Harper MA, Collen J. 2002.Glaciations, interglaciations and reworked microfossils in Poukawa Basin, New Zealand.*Global and Planetary Change***33**: 43–256.

Hayward B, Grenfell HR, Sabaa AT, Carter R, Cochran U, Lipps JH, Shane PR, Morley M. 2006. Micropaleontological evidence of large earthquakes in the past 7200 years in southern Hawke's Bay, New Zealand. *Quaternary Science Reviews* **25**: 1186-1207.

Hicks DM, Shankar U. 2003. Sediment yield from New Zealand rivers. *NIWA Chart, Miscellaneous Series***79**.

Hull AG. 1985. *Late Quaternary geology of the Cape Kidnappers area, Hawke's Bay, New Zealand*. MSc thesis, Victoria University, Wellington, New Zealand.

Hull AG. 1986. Pre-A.D. 1931 tectonic subsidence of Ahuriri Lagoon, Napier, Hawke's Bay, New Zealand.*New Zealand Journal of Geology and Geophysics* **29**: 75-82.

Hull AG. 1987. A late holocene uplifted shore platformon the Kidnappers coast, North Island, New Zealand: some implications for shore platform development and uplift mechanism. *Quaternary Research***28**: 183–195.

Imbrie J, Hays JD, Martinson DG, McIntyre A, Mix AC, Morley JJ, Pisias NG, Prell WL, Shackleton NJ, 1984. The orbital theory of Pleistocene climate: support from a revised chronology of the marine $\delta^{18}O$ record. In: Berger A, Imbrie J, Hays J, Kukla G, Saltzman B. (Eds.), Milankovitch and climate. Reidel Publishing Company, Dordrecht, pp. 269-305.

Jervey MT. 1988. Quantitative geological modeling of siliciclastic rock sequences and their seismic expression. In Sea-level Changes—An Integrated Approach, Wilgus CK, Hastings BS, Kendall ChStCG, Posamentier HW, Ross CA, Van Wagoner JC (eds). Special Publication 42, Society Economic Paleontologists Mineralogists: Tulsa, OK: 47-69.

Kamp PJJ. 1978. *Stratigraphy and sedimentology of conglomerates in the Pleistocene Kidnappers Group, Hawkes Bay*. Unpublished MSc thesis, University of Waikato, Hamilton, New Zealand

Kamp PJJ. 1990. Kidnappers Group (middle Pleistocene), Hawke's Bay. *Geological Society of New Zealand miscellaneous publication* **50B**: 105-118.

Kingma JT, 1958. Geology of the Wakarara Range, central Hawke's Bay.*New Zealand Journal of Geology and Geophysics* **1**, 76-91.

Kingma JT. 1971. Geology of the Te Aute subdivision. *New Zealand Geological Survey Bulletin***70**: 173 pp.

Lamarche G, Barnes PM, Bull JM. 2006. Faulting and extension rate over the last 20,000 years in the offshore Whakatane Graben, New Zealand continental shelf. *Tectonics* **25**: TC4005 doi: 10.1029/2005TC001886.

Lee HJ, Syvitski JPM, Parker G, Orange D, Locat J, Hutton EWH, Imram J. 2002. Distinguishing sediment waves from slope failure deposits: field examples, including the 'Humboldt Slide', and modelling results. *Marine Geology***192**: 79-104.

Lewis KB. 1971a. Growth rate of folds using tilted wave planed surfaces: coast and continental shelf, Hawke's Bay, New Zealand. *In*: Collins, B. W.; Fraser, R. *ed*. Recent crustal movements. *The Royal Society of New Zealand Bulletin* **9**: 225-231.

Lewis KB. 1971b. Slumping on a continental slope inclined at *l°-4°*. *Sedimentology* **16**:97-110.

Lewis KB. 1973a. Erosion and deposition on a tilting continental shelf during Quaternary oscillations of sea level.*New Zealand journal of geology and geophysics* **16**: 281-301.

Lewis KB. 1973b. Sediments on the continental shelf and slope between Napier and Castelpoint, New Zealand.*New Zealand journal of marine and freshwater research***7**: 183-208.

Lewis KB. 1974. Upper Tertiary rocks from the continental shelf and slope of Southern Hawke's Bay. *New Zealand journal of marine and freshwater research***8**: 663-670.

Lewis KB. 1980. Quaternary sedimentation on the Hikurangi oblique-subduction and transform margin, New Zealand. In *Sedimentation in oblique slip mobile zone*, Ballance, P.F., Reading, H.G. (eds). Special publication International Association of Sedimentologists **4**: 171-189.

Lewis KB, Bennett DJ. 1985. Structural pattern on the Hikurangi Margin: an interpretation of new seismic data. in*New seismic profiles, cores, and dated rocks from the Hikurangi margin, New Zealand*, Lewis, K.B. (comp). New Zealand Oceanographic Institute field report **22**. Division of Marine and Freshwater Science, Department of Scientific and Industrial Research, Wellington.

Lewis KB, Pettinga JR. 1993. The emerging, imbricate frontal wedge of the Hikurangi margin. *In*: South Pacific sedimentary basins. *Sedimentary Basins of the World 2*, *Basins of the Southwest Pacific*, Ballance PF (ed.). Elsevier, Amsterdam: 225–250.

Lewis KB, Collot J-Y, Davy BW, Delteil L, Lallemand SE, Uruski CI & GeodyNZ team. 1997. North Hikurangi GeodyNZ swath maps: depth, texture and geological interpretation. *NIWA chart miscellaneous series***72**. National Institute of Water and Atmospheric Research, Wellington.

Lian O, Shane P. 2000. Optical dating of paleosols bracketing the widespread Ratoehu tephra, North Island, New Zealand.*Quaternary Science Review***19**: 1649-1662.

Lisiecki LE, Raymo ME. 2005. A Pliocene-Pleistocene stack of 57 globally distributed benthic $\delta^{18}O$ records. *Paleoceanography* **20**: PA1003, doi:10.1029/2004PA001071.

Litchfield N. 2003. Maps, stratigraphic logs and age control data for river terraces in the eastern North Island. *Institute of Geological and Nuclear Sciences Science Report* **31**: 102 pp.

Litchfield NJ, Berryman KR. 2005. Correlation of fluvial terraces within the Hikurangi Margin, New Zealand: Implications for climate and base level controls. *Geomorphology***68**: 291-313.

Litchfield NJ, Berryman KR. 2006. Relations between postglacial fluvial incision rates and uplift rates in North Island, New Zealand. *Journal of Geophysical Research* **111**: doi:10.1029/2005JF000374.

Litchfield N, Rieser U. 2005. OSL age constraints for fluvial aggradation terraces and loess in the eastern North Island, New Zealand, *New Zealand Journal of Geology and Geophysics***48**: 581-589.

Lu H, Fujthorpe CS, Mann P, Michelle AK. 2005. Miocene-Recent tectonic and climatic controls on sediment supply and sequence stratigraphy: Canterbury basin, New Zealand. *Basin Research***17**: 311-328. doi: 10.1111/j.1365-2117.2005.00266.x.

Marutani T, Kasai M, Reid LM, Trustrum NA. 1999. Influence of storm-related sediment storage on the sediment delivery from tributary catchments in the upper Waipaoa River, New Zealand. *Earth Surface Processes and Landforms***24**: 881–896.

McArthur JL, Shepherd MJ. 1990. Late Quaternary glaciation of Mt Ruapehu, North Island, New Zealand. *Journal of The Royal Society of New Zealand* **20**:287-296.

McGlone MS. 2001. A late Quaternary pollen record from marine core P69, southeastern North Island, New Zealand.*New Zealand Journal of Geology and Geophysics***44**: 69-77.

McGlone MS. 2002. The late Quaternary peat, vegetation and climate history of the Southern Oceanic Islands of New Zealand.*Quaternary Science Reviews***21**: 683-707.

McGlone MS, Howorth R, Pullar WA. 1984. Late Pleistocene stratigraphy, vegetation and climate of the Bay of Plenty and Gisborne regions, New Zealand. *New Zealand Journal of Geology and Geophysics***27**: 327-350.

McLea WL. 1990. Palynology of the Pohehe Swamp, northwest Wairarapa, New Zealand: a study of climatic and vegetation changes during the last 41 000 years. *Journal of the Royal Society of New Zealand***20**: 205-220.

Miall AD. 1991. Stratigraphic sequences and their chronostratigraphic correlation. *Journal of Sedimentary Petrology***61**: 497-505.

Milliman JD, Syvitski JPM. 1992. Geomorphic tectonic control of sediment discharge to the ocean: the importance of small, mountainous rivers. *Journal of Geology* 100: 525-544.

Multiwave. 2005. 05CM 2D Seismic Survey, Offshore East Coast - North Island. New Zealand unpublished openfile petroleum report 3136. Ministry of Economic Development, Wellington.

Naish TR, Field BD, Zhu H, Melhuish A, Carter RM, Abbott ST, Edwards S, Alloway BV, Wilson GS, Niessen F, Barker A, Browne GH, Maslen G. 2005. Integrated outcrop, drill core, borehale and

seismic stratigraphic architecture of a cyclothemic, shallow-marine depositional system, Wanganui Basin, New Zealand. *Journal of the Royal Society of New Zealand***35**: 91-122.

Newnham RM, Lowe DJ, Williams PW. 1999. Quaternary environmental change in New Zealand: a review. *Progress in Physical Geography***23**: 567-610.

Newnham RM, Lowe DJ. 2000. Fine–resolution pollen record oflate-glacia l climate reversal from New Zealand. *Geology***28**: 759-762.

Newnham RM, Eden DN, Lowe DJ, Hendy CH. 2003. Rerewhakaaitu Tephra, a land-sea marker for the last termination in New Zealand with implications for global climatic change. *Quaternary Science Reviews***22**: 289–308.

Nicol A, Mazengarb C, Chanier F, Rait G, Uruski C, Wallace L. 2007 Tectonic evolution of the active Hikurangi subduction margin, New Zealand, since the Oligocene. *Tectonics* **26**: doi:10.1029/2006TC 002090

Okamura Y, Blum P. 1993. Seismic stratigraphy of Quaternary stacked progradational sequences in the southwest Japan forearc: an example of fourth-order sequences in an active margin, Sequence Stratigraphy and Facies Associations. *International Association of Sedimentologists, Special Publication***18**: 213-232.

Okuda M, Shulmeister J, Flenley JR. 2002. Vegetation changes and their climatic implications for the late Pleistocene at Lake Poukawa, Hawkes Bay. *Global and Planetary Change***33**: 269-282.

Orpin AR. 2004. Holocene sediment deposition on the Poverty-slope margin by the muddy Waipaoa River, East Coast New Zealand. *Marine geology***209**: 69-90.

Orpin AR, Alexander C, Carter L, Kuehl S, Walsh JP. 2006. Temporal and spatial complexity in post-glacial sedimentation on the tectonically active, Poverty Bay continental margin of New Zealand. *Continental Shelf Research***26**: 2205-2224.

Pahnke K, Sachs JP. 2006. Sea surface temperatures of southern midlatitudes 0-160 kyr B.P. *Paleoceanography***21**: PA2003, doi:10.1029/2005PA001191.

Pantin HM. 1966. Sedimentation in Hawke Bay. *New Zealand Department of Scientific and Industrial Research bulletin* **171**:70 pp.

Paquet F. 2007. Morphostructural evolution of active subduction margins: The example of the Hawke bay Forearc Basin, New Zealand. PhD Thesis, Universite de Rennes 1, Rennes, France *and* University of Canterbury, Christchurch, New Zealand, 253pp.

Payton CE. 1977. *Seismic Stratigraphy – applications to hydrocarbon exploration*. American Association of Petroleum Geologist Memoir **26**: 516 pp.

Pettinga JR. 1982. Upper Cenozoic structural history, coastal southern Hawke's Bay, New Zealand. *New Zealand journal of geology and geophysics***25**: 149-19 1.

Pillans B. 1986. A late Quaternary uplift map for North Island, New Zealand. In *Recent crustal movements of the Pacific region*, Reilly, W.l., Harford, B.E. (eds). Royal Society of New Zealand bulletin **24**: 409-417.

Pillans B, McGlone M, Palmer A, Mildenhall D, Alloway B, Berger G. 1993. The Last Glacial Maximum in central and southern North Island, New Zealand: a paleoenvironmental reconstruction using Kawakawa Tephra Formation as a chronostratigraphic marker. *Palaeogeography Palaeoclimatology Palaeoecology* **101**: 283-304.

Posamentier HW, Jervey MT, Vail PR. 1988. Eustatic controls on clastic deposition I-Conceptual framework. In *Sea-level Changes—an Integrated Approach*, Special Publication 42, Wilgus CK, Hastings BS, Kendall ChStCG, Posamentier HW, Ross CA, Van Wagoner JC (eds). Society Economic Paleontologists Mineralogists: Tulsa, OK; 109-124.

Posamentier HW, Vail PR. 1988. Eustatic controls on clastic deposition II-Sequence and systems tract models. In *Sea-level Changes—an Integrated Approach*, Wilgus CK, Hastings BS, Kendall ChStCG, Posamentier HW, Ross CA, Van Wagoner JC (eds). Special Publication 42, Society Economic Paleontologists Mineralogists: Tulsa, OK; 125-154.

Posamentier HW, Allen GP, James DP, Tesson M. 1992. Forced regressions in a sequence stratigraphic framework: concepts, examples and exploration significance. *American Association of Petroleum Geologists Bulletin* **76**: 1687-1709.

Proust J-N, Chanier F. 2004. The Pleistocene Cape Kidnappers section in New Zealand : orbitally forced controls on active margin sedimentation? *Journal of Quaternary Science***19**: 591-603.

Proust J-N, Lamarche G, Nodder S, Kamp PJJ. 2005. Sedimentary architecture of a Plio-Pleistocene proto-back-arc basin: Wanganui, New Zealand. *Sedimentary Geology***181**: 107-145.

Proust J-N, Lamarche G, Migeon S, Neil H, and Shipboard party. 2006. MD152 / MATACORE "Tectonic and climate controls on sediment budget". *Les rapports de campagnes à la mer* : pp. 107.

Pullar WA, Heine JC. 1971. Ages, inferred from ^{14}C dates, of qome tephra and other deposits from Rotorua, Taupo, Bay of Plenty, Gisborne and Hawkes Bay districts. *Proceedings of radiocarbon users conférence*, Wellington : 117-138.

Raub ML. 1985. *The neotectonic evolution of the Wakarara area*, M.Sc. thesis, Auckland Univ., Auckland, New Zealand: pp. 122.

Ridgway NM. 1960. Surface water movements in Hawke Bay, New Zealand. *New Zealand journal of Geology and Geophysics* **3**(2): 253-261.

Ridgway NM, Stanton BR. 1969. Some hydrological features of Hawke Bay and nearby shelf waters. *New Zealand journal of marine and freshwater research***3**: 545-559.

Saul G, Naish TR, Abbot ST, Carter RM.1999. Sedimentary cyclicity in the marine Pliocene-Pleistocene of the Wanganui basin (New Zealand): Sequence stratigraphic motifs characteristic of the past 2.5 m.y. *Geological Society of America Bulletin***111**: 524-537.

Shane PAR. 1994. A widespread, early Pleistocene tephra (Potaka tephra, 1 Ma) in New Zealand: Character, distribution, and implications. *New Zealand Journal of Geology and Geophysics* **37**:25-35.

Shane PAR, Black TM, Alloway BV, Westgate JA 1996. Early to middle Pleistocene tephrochronology of North Island, New Zealand: implications for volcanism, tectonism, and paleoenvironments. *Geological Society of America Bulletin***108**: 915–925.

Shane P, Sandiford A. 2003. Paleovegetation of marine isotope stages 4 and 3 in Northern New Zealand and the age of the widespreade Rotoehu tephra. *Quaternary Research***59**: 420-429.

Sheriff RB. 1980: *Seismic Stratigraphy*. IHRDC, Boston: 227pp.

Shulmeister J, Shane P, Lian OB, Okuda M, Carter JA, Harper M, Dickinson WW, Augustinus P, Heijnis H. 2001. A long late-Quaternary record from Lake Poukawa, Hawkes Bay, New Zealand.*Palaeogeography Palaeoclimatology Palaeoecology***176**: 81– 107.

Shulmeister J, Goodwin I, Renwick J, Harle K, Armand L, McGlone MS, Cook E, Dodson J, Hesse PP, Mayewski P, Curran M. 2004. The Southern Hemispher westerlies in the Australasian sector over the last glacial cycle: a synthesis. *Quaternary International* **118-119**: 23-53.

Shumm SA. 1993. River Response to Baselevel Change: Implications for Sequence Stratigraphy. *The journal of Geology* **101**: 279-294.

Smale D, Houghton BF, McKellar IC, Mansergh GD, Moore PR. 1978. Geology and erosion in the Ruahine Range: a reconnaissance study. In *Geology and erosion in the Ruahine Range*, Speden, I. (ed.).*New Zealand Geological Survey Report* **G20**: 7-30.

Spörli KB, Ballance PF. 1989. Mesozoic-Cenozoic ocean floor-continent interaction and terrane configuration, southwest Pacific area around New Zealand. In. *Mesozoic and Cenozoic evolution of the Pacific Ocean margins*, Ben Avraham Z. (ed.). Oxford University Monograph, geology and geophysics **8**: 176-190.

Strong N, Paola C. 2006. Fluvial Landscapes and Stratigraphy in a Flume. *The Sedimentary Record***4**: 4-8.

Sullivan D. 1990. 2D Marine Seismic Survey Acquisition Report PPL 38322, PPL 38321. New Zealand unpublished open-file *Petroleum Report***1666**. Ministry of Economic Development, Wellington.

Talling PJ. 1998. How and where do incised valleys form if sea level remains above the shelf edge? *Geology* **26**: 87-90.

Vail PR, Mitchum JR, Todd RG, Widmier JM, Thompson S, Sangree JB, Bubb JN, Hatlelid WG. 1977. Seismic Stratigraphy and Global Changes of Sea Level in Depositional Sequences. In *Seismic Stratigraphy – applications to hydrocarbon exploration*, Payton E (Ed). American Association of Petroleum Geologist Memoir **26**: 49-212.

Van Wagoner JC, Posamentier HW, Mitchum RM, Vail PR, Sarg JF, Loutit TS, Hardenbol J, 1988.An overview of fundamentals of sequence stratigraphy and Key definitions.*In Sea-level Changes—an Integrated Approach*, Wilgus CK, Hastings BS, Kendall ChStCG, Posamentier HW, Ross CA, Van Wagoner JC (eds). Special Publication **42**, Society Economic Paleontologists Mineralogists: Tulsa, OK; 39-45.

Waelbroeck C, Labeyrie L, Michel E, Duplessy JC, McManus JF, Lambeck K, Balbon E, Labracherie M. 2002. Sea-level and deep water temperature changes derived from benhic foraminifera isotopic records. *Quaternary Science Reviews***21**: 295-305.

Wilmhurst JM, McGlone MS, Leathwick JR, Newnham RM. 2007. A pre-deforestation pollen-climate calibration model for New Zealand and quantitative temperature reconstructions for the past 18 000 years BP. *Journal of Quaternary Science* **22**: 535-547.

Wilson CJN, Houghton BF, Lanphere MA, Weaver SD. 1992. A new radiometric age estimate for the Rotoehu Ash from Mayor Island volcano, New Zealand. *New Zealand Journal of Geology and Geophysics***35**: 371–374.

Woolfe KJ, Larcombe P, Naish T, Purdon RG. 1998. Lowstand rivers need not incise the shelf: an example from the Great Barrier Reef, Australia, with implications for sequence stratigraphic models. *Geology***26**: 75–78.

Wright IC, Lewis KB. 1991. Seafloor sampling as a window to deeper structure along offshore accretionary systems: an example from offshore East Coast, North Island, New Zealand. *Proceedings of 1991 New Zealand Oil Exploration Conference* **1**: 101-109.

TABLES

Table 1:

Characteristics of the 6 seismic units (upper and lower boundaries and seismic facies) recognised on seismic data covering the offshore Hawke's Bay forearc domain.

Table 2:

Characteristics of the 11 seismic facies recognised on seismic data covering the offshore Hawke's Bay forearc domain with description, interpretation in sedimentary facies and examples in MCS, Boomer and/or 3.5 KHz data.

FIGURE CAPTIONS

Figure 1:

Tectonic setting of the active Hikurangi subduction margin. (A) Australian-Pacific plate boundary in the New Zealand region. Light gray shading corresponds to submerged continental crust and dark gray shading represents the emergent continental crust of the New Zealand micro-continent. (B) Arrangement of the major morphostructural elements of the Hikurangi subduction margin in the North Island including the Hikurangi Trough, the imbricate frontal wedge emergent in the coastal ranges, the Neogene forearc basin domain, the axial ranges of the Frontal Ridge, backarc basin and Pleistocene volcanic arc. The dashed line A-A' corresponds to the trace of the crustal cross section. (C) Crustal cross section A-A' modified from Beanland (1995), Begg et al. (1996) and Barnes et al. (2002) showing the structure of the central part of the subduction margin. RF: Ruahine Fault; MF: Mohaka Fault; KR: Kidnappers Ridge; LB: Lachlan Basin; LR: Lachlan Ridge; MR: Motu-o-Kura Ridge. (D) Map showing the main morphostructural elements in the Hawke's Bay region.

Figure 2:

Location map of seismic surveys, long piston cores and wells used for this study. Seismic profiles and topographic sections that appear in figures (sections) are respectively in bold solid and dashed black lines with reference to the figure.

Figure 3:

Map showing the current onshore (Hawke's Bay) and offshore (Hawke Bay) morphology and the main tectonic structures. The bathymetry contours and digital elevation model are from Collot et al. (1996), Lewis et al. (1997) and unpublished data acquired by NIWA. The onshore topographic elevations and digital elevation model are derived from the NZTopo Map Series (Land Information New Zealand). Location of the calypso core MD97-2121 is provided here (Carter and Manighetti, 2006).

Figure 4:

Schematic sections across the submerged Hawke's Bay sector of the forearc domain showing the general geometry of the seismic units and unconformities described in this study. (A) Location map for cross sections in (B) and (C). Abbreviations: KB - Kidnappers Basin; MaB - Mahia Basin; LB - Lachlan Basin; MoB - Motu-o-Kura Basin; LPS – Late Pleistocene Sequence; S – major unconformities; U – seismic unit. (B) Cross section parallel to the slope and passing over the active uplifting Kidnappers ridge. U6 and U5 are the only seismic units that can be traced over the ridge in the southern part of Hawke Bay. (C) Cross section extending around the north end of the active Kidnappers ridge and passing through other major subsiding basins. All seismic units, excepted U4, can be traced from the onshore area to the upper slope area (c. 500 m water depth).

Figure 5:

Interpretation of the inner shelf Boomer profiles from the GSR 05301 survey, showing uninterpreted processed data with seismic facies labels (referring to Table 2) and the corresponding interpretation with unconformities (S1 to S5) and seismic units (U1 to U6) for (A) line 11, (B) line 8 and (C) line 6

(for locations refer to Fig. 2). The vertical exaggeration is approximately x45. The legend (D) shows the interpretation of seismic units as system tracts and their correlation to the stratigraphic time chart.

Figure 6:

Interpretation of the outer shelf to upper slope 3.5 KHz profile from MD 152 survey (Proust et al., 2006; see location map - Fig. 2), showing uninterpreted profile with seismic facies labels (Fs8 to Fs 11) and the corresponding interpretation with unconformities (S1, S2, S4, and S5), seismic units (U1b, U2, U3, U5 and U6). The legend shows the interpretation of seismic units as system tracts and their correlation to the stratigraphic time chart. On the northwestern part, unconformity S1 is projected from multi-channel seismic profiles #05 from TAN 0313 survey and #28 from 05CM survey (Multiwave 2005; see S1 on Fig. 9). Cores S783, S784, Q939 and Q942 (Barnes et al., 1991) are orthogonally projected southward on the profile of c.500m. The vertical exaggeration is approximately x35 with depth conversion assuming an average velocity in the water column of 1500 $m.s^{-1}$. The magnification of the profile on the upper right shows the continuity (arrows) of some acoustic reflections through the "fault-like", weakly reflective zones.

Figure 7:

Interpretation of the inner to outer shelf 3.5 KHz profile AG#1 from AG&S survey (Conquest Exploration 1988; see location map - Fig. 2), showing raw data profile and the corresponding interpretation with unconformities (S1 to S5) and seismic units (U1 to U6). Insert shows the interpreted boomer line 8 that allows correlation between the inner and outer shelf. The location of LGM shoreline is indicative and corresponds to the lower limit of sub-aerial erosion-like features visible immediately westward, on which postglacial deposits show transgressive onlaps. It is also in accordance with the documented LGM sealevel at c. -120m, corrected from local tectonic uplift (Imbrie et al., 1984; Waelbroeck et al., 2002). The vertical exaggeration is approximately x100.

Figure 8:

Lithological logs of Tollemache Orchard and Awatoto wells (for locations refer Fig. 2), modified from Dravid and Brown (1997). The figure depicts the evolution of the interpreted depositional environments, the position of dated samples, and the proposed correlation to both the seismic stratigraphy from Boomer interpretations and the oxygen isotope stratigraphy and curve (Lisiecki and Raymo 2005; Waelbroeck et al. 2002; Imbrie et al. 1984). The correlation to the oxygen isotope stratigraphy is based on: (1) available dated samples; (2) the succession of depositional environments that fit to the trends observed on the oxygen isotope curve; and (3) the occurrence of marine deposits at the base of the section that we assume to be last interglacial in age. 4^{th} and 5^{th} order sequence stratigraphy is proposed with black and white triangles and grey rectangles figuring respectively prograding, retrograding and aggrading phases.

Figure 9:

Interpretation of the outer shelf to upper slope multi-channel seismic profiles #29 (A) and #41 (B) from the 05CM survey (Multiwave 2005; see location map - Fig. 2), showing the migrated profile and the corresponding interpretation with unconformities (S1, S2, S4, and S5) and seismic units (U1, U2, U3, U5 and U6). Dashed and solid bold lines correspond respectively to maximum flooding surfaces and sequence boundaries. Landward and seaward stepping trends within LPS1 are indicated. The vertical exaggeration is approximately x10.

Figure 10

Geometric correlation between surface S1 identified on high resolution Boomer profiles and the uplifted 120 ka marine terrace overlying the Pleistocene Kidnappers Group in the southern Hawke Bay coastal area. (A) Map showing the isocontours of S1 as determined from Boomer profile (values in meters bsl), the remnants of the uplifted 120 ka marine terrace as identified from geological mapping, and the location of the section XX' (B) and the position and orientation of the picture (C). (B)**:** XX' section showing the geometric correlation between S1 and the strath surface of the 120 ka marine terrace using Boomer interpretations, topographic data and geological mapping. (C) Photograph of the coastal cliffs of southern Hawke Bay, taken 1 km SW from Black Reef and looking to the West. The

photo shows the almost flat surface of the uplifted 120 ka marine terrace overlying the NW tilted Pleistocene Kidnappers Group (Photo by F. Paquet).

Figure 11:

Topographic sections across the foothills domain (see location map – Fig. 2) that summarize the occurrence of the major fluvial terraces. (A) transverse profile across major southern Hawke's Bay river valleys (Tukituki, Waipawa, Makaroro and Ngaruroro) showing: the location of age calibrated fluvial terraces T1, T2 and T3 (from Litchfield and Berryman 2005), the location of undated older terraces (T4 and Salisbury terrace), the uplift rate estimations U (from Litchfield and Berryman 2006) and the stratigraphic log of the Pleistocene substratum (Makaroro section) with age calibrated tephras (Shane 1994). (B) Longitudinal profiles of the river bed (RB) terraces, T1, T3 and T4 along the Ngaruroro valley and corresponding uplift rate estimations using method from Litchfield and Berryman (2006).

Figure 12:

(A) Age estimation of undated older terraces T4 and Salisbury, using their elevation at the same point of the stream profile, assuming constant uplift rates (U) and similar conditions of formation. (B) Correlation of fluvial aggradation periods within valleys to the oxygen isotope stratigraphy and mean sea level curve (Lisiecki and Raymo 2005; Waelbroeck et al. 2002; Imbrie et al. 1984) using age calibrated samples (Litchfield and Berryman, 2005; Litchfield and Rieser, 2006) and age estimation of the T4 and Salisbury terraces.

Figure 13:

Schematic sections across the Hawke's Bay forearc domain depicting the "source to sink" interpretation of seismic units (U2 to U6) and fluvial terraces (T1 to Salisbury, on section B) as system tracts and the correlation to the oxygen isotope stratigraphy and mean sea level curve (Lisiecki and Raymo 2005; Waelbroeck et al. 2002; Imbrie et al. 1984). (A) Cross section parallel to the slope and passing over the actively uplifting Kidnappers ridge. (B) Cross section extending around the north end

of the Kidnappers ridge and passing through the major subsiding basins, from the axial range front to the upper slope area (~500 m water depth). For location of sections refer to Fig. 4. Abbreviations in (C): SB: Sequence boundary; MFS: Maximum Flooding Surface; LPS: Late Pleistocene Sequence.

Figure 14:

Schematic sections across the Hawke's Bay forearc domain depicting the "source to sink" interpretation of seismic units (U2 to U6) and fluvial terraces (T1 to Salisbury - section B) as sedimentary facies and depositional environments (See text for details). (A) cross section parallel to the slope and passing over the active uplifting Kidnappers ridge. (B) cross section extending around the north end of Kidnappers ridge and passing through the major subsiding basins, from the axial range front to the upper slope area (c. 500 m water depth). For location of sections refer to Fig. 4.

Figure 15:

Isopach map of the late Pleistocene sequence LPS1 (~150 to 30 ka) as identified from seismic interpretation. Two-way travel times were converted to depth, then thickness, using an average velocity of 1600 $m.s^{-1}$. Isopach contours have been digitized and the map has been generated in GIS software. The four main depocenters are located and designated by the following abbreviations: KB: Kidnappers Basin; MaB: Mahia Basin; LB: Lachlan basin; MoB: Motu-o-Kura Basin. Aggradational terraces of LPS1 (T2, T3, T4 and Salisbury) are mapped but not differentiated. Active and inferred tectonic structures are superimposed in order to reveal the impact of tectonic deformation on the distribution of sediments. The volume of LPS1 sediments deposited and preserved reaches ~340 km^3.

Figure 16:

Isopach map of the late Pleistocene sequence LPS2 (30 ka to present) as identified from seismic interpretation. Two-way travel times were converted to depth, then thickness, using an average velocity of 1600 $m.s^{-1}$. Isopach contours have been traced from our seismic interpretation and completed from previous studies for the northern Hawke's Bay area (Wright and Lewis 1991) and the Poverty shelf (Foster and Carter 1997; Orpin et al. 2006). Contours have been digitized and the map

has been generated in GIS software. The four main depocenters are located and designated by the following abbreviations: KB: Kidnappers Basin; MaB: Mahia Basin; LB: Lachlan basin; and MoB: Motu-o-Kura Basin. Aggradational terraces (T1) are also shown. Active and inferred tectonic structures are superimposed in order to reveal the strong impact of tectonic deformation on the distribution of sediments. The volume of LPS2 sediments deposited and preserved reaches ~140 km^3. The heavy white dashed line delineates the mid-shelf HST depocenter inboard of the Waimarama thrust zone, and the heavy black dashed line delineates the linked shelf to upper slope Lachlan – Motu-o-Kura LST depocentre.

Figure 17:

Paleogeographic reconstructions for the late Pleistocene environmental extremes that integrate results from seismic interpretation, piston-cores, onshore and offshore wells and mapping, as well as results from previous studies (Ridgway 1960; Pantin 1966; Ridgway and Stanton 1969; Lewis 1973a,b; Carter 1974; Smale et al. 1978; Grant-Taylor 1978; Francis 1985; Hull 1985, 1986; Lewis and Barnes 1991; Barnes et al. 1991; Dravid and Brown 1997; Carter et al. 1998; Carter 2001; Shulmeister et al. 2001; Harper and Collen 2002; Okuda et al. 2002; Litchfield 2003; Litchfield and Berryman 2006; Hayward et al. 2006; Cochran et al. 2006; Proust et al. 2006; this study): (A): Reconstruction of the distribution of depositional environments within the forearc domain study area during the Last Glacial Maximum (c. 20 ka). The position of braided channels are schematically shown, based on our facies interpretations. (B) Reconstruction of the distribution of depositional environments within the forearc domain study area during the Holocene optimum (c. 7.2 ka). Abbreviations include: KB: Kidnappers Basin; MaB: Mahia Basin; LB: Lachlan basin; and MoB: Motu-o-Kura Basin.

APPENDIX

Appendix 1:

Description of the data set interpreted or used in this study.

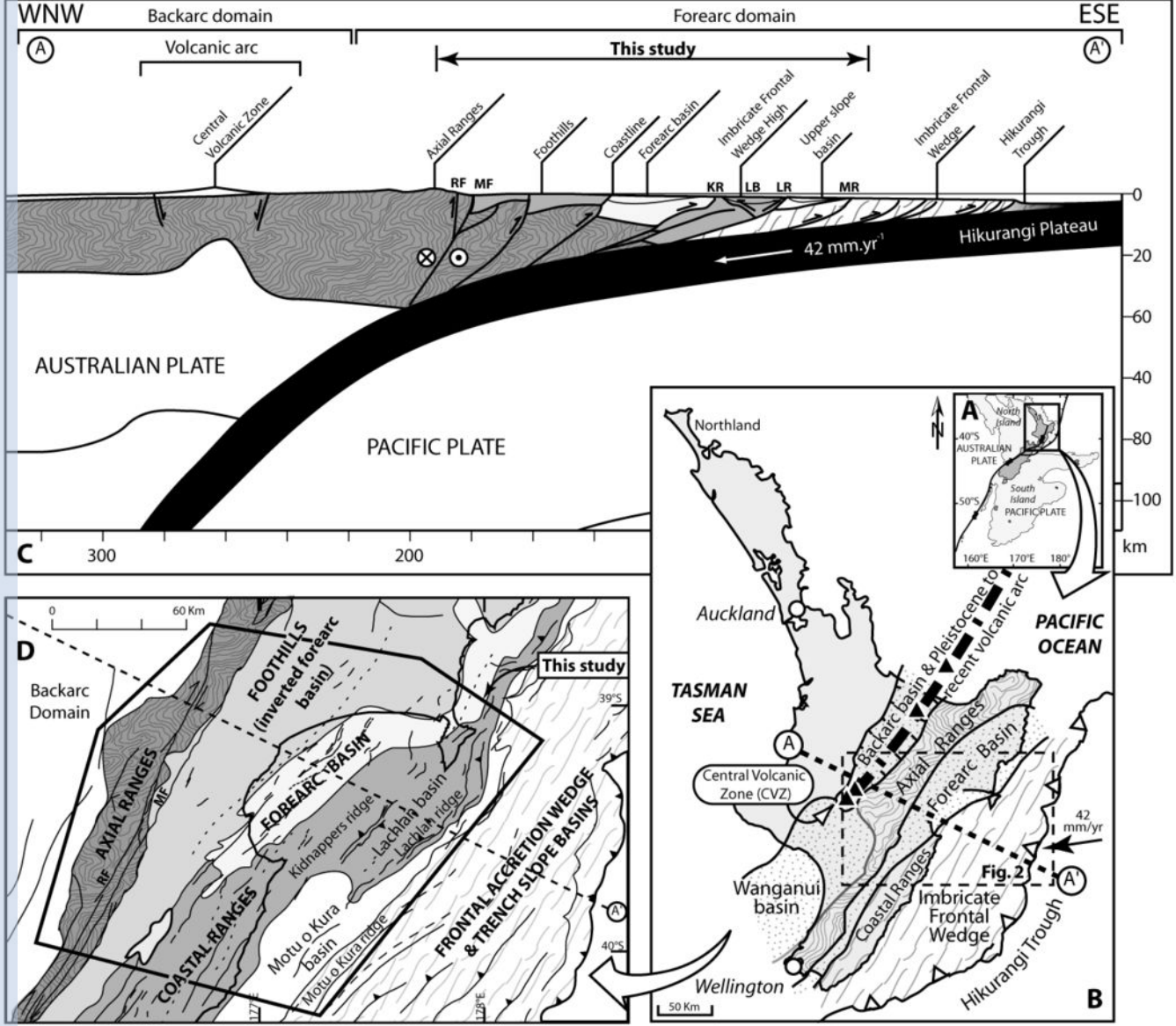

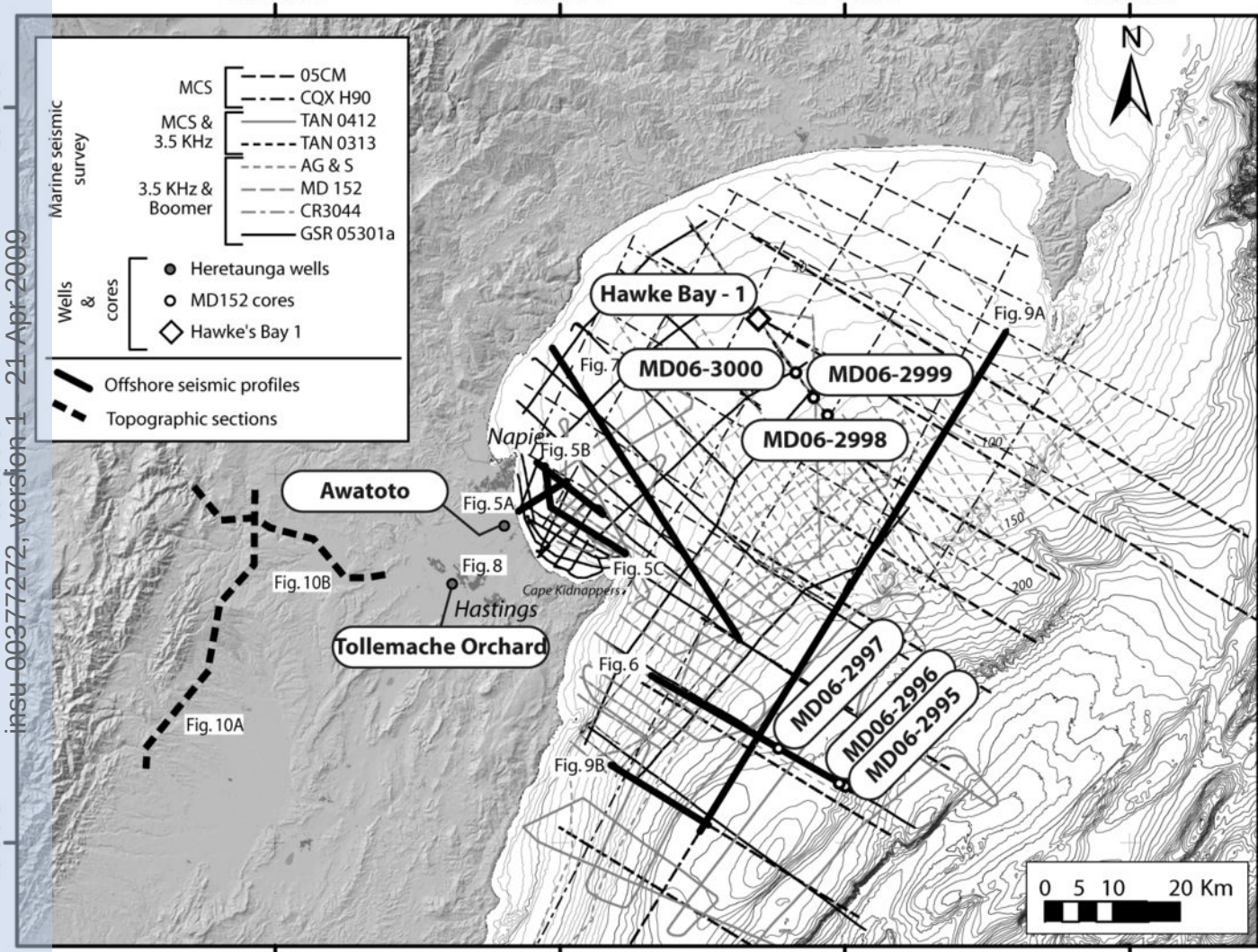

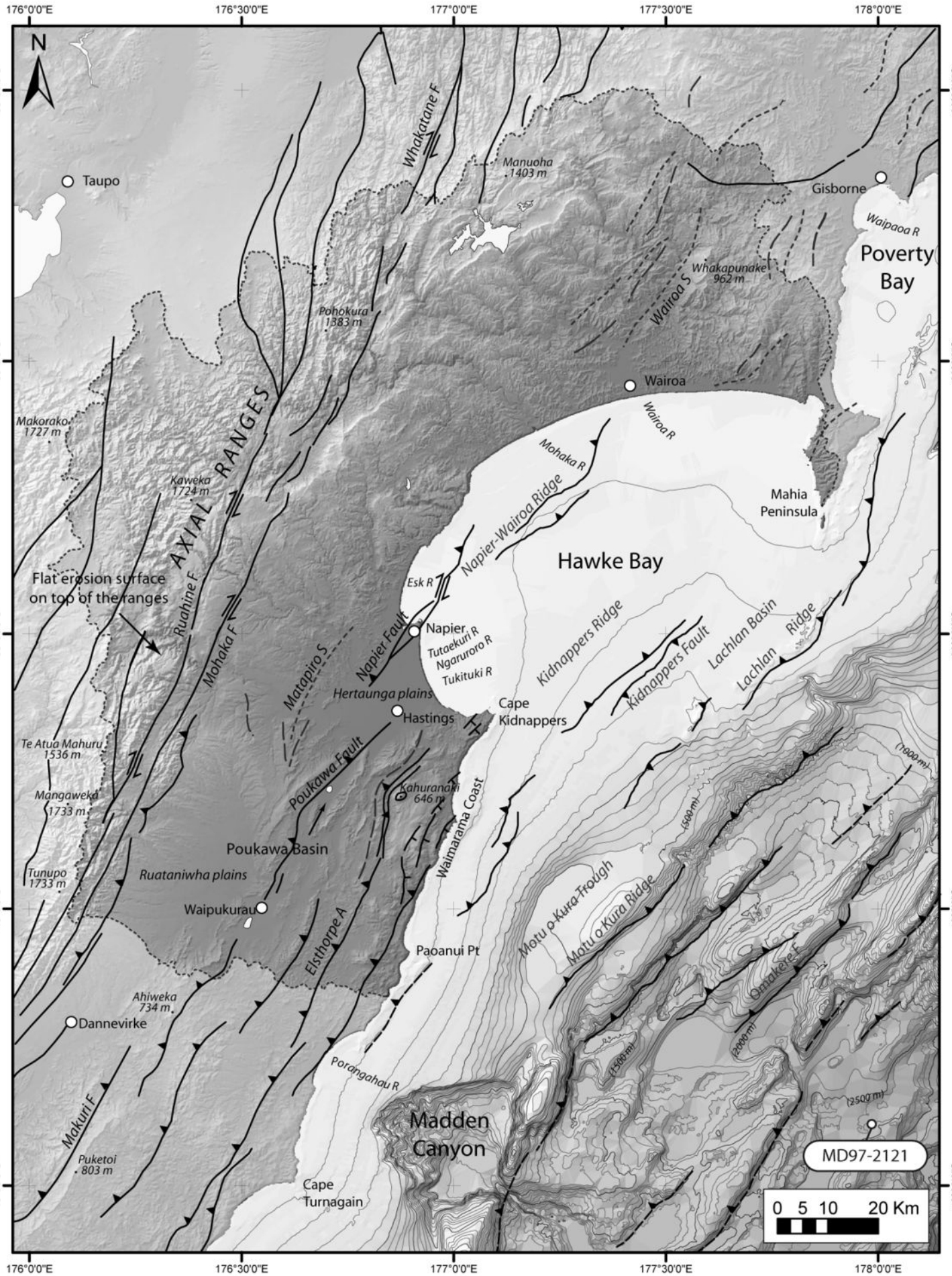

Legend:

- Thrust fault
- Inferred thrust fault
- Syncline (S)
- Anticline (A)
- Normal fault
- Dextral strike -slip fault
- Limit of the Hawke's Bay drainage basin
- Main town

Bathymetric contours every 50 m

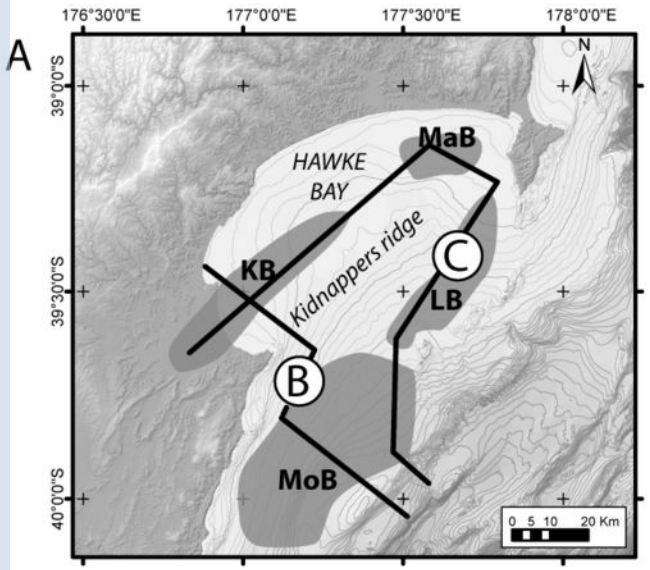

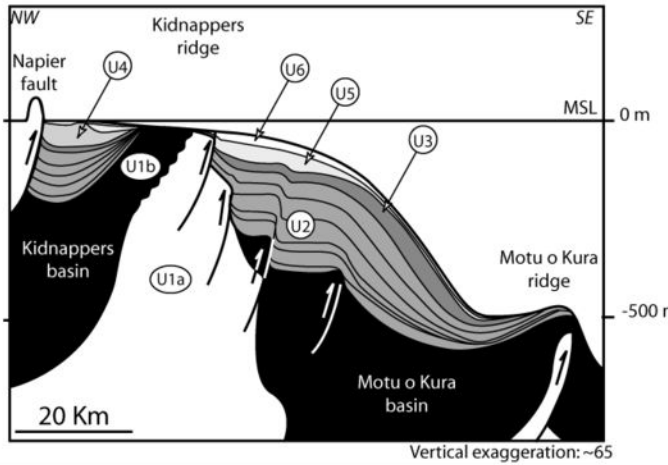

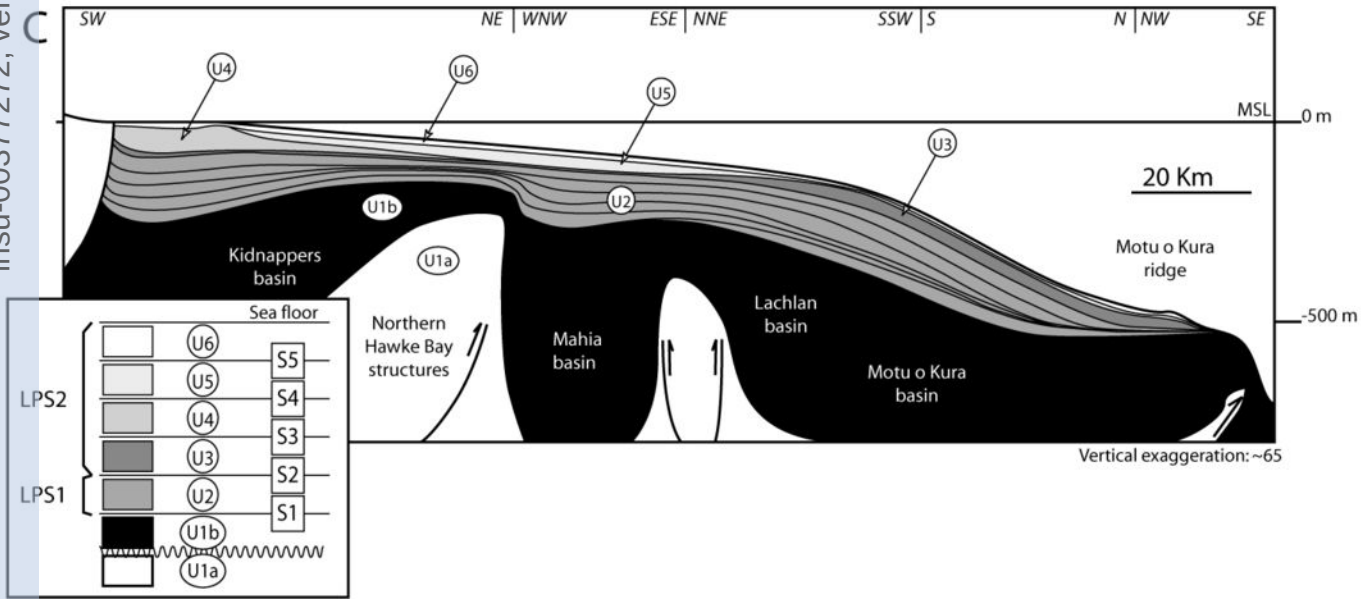

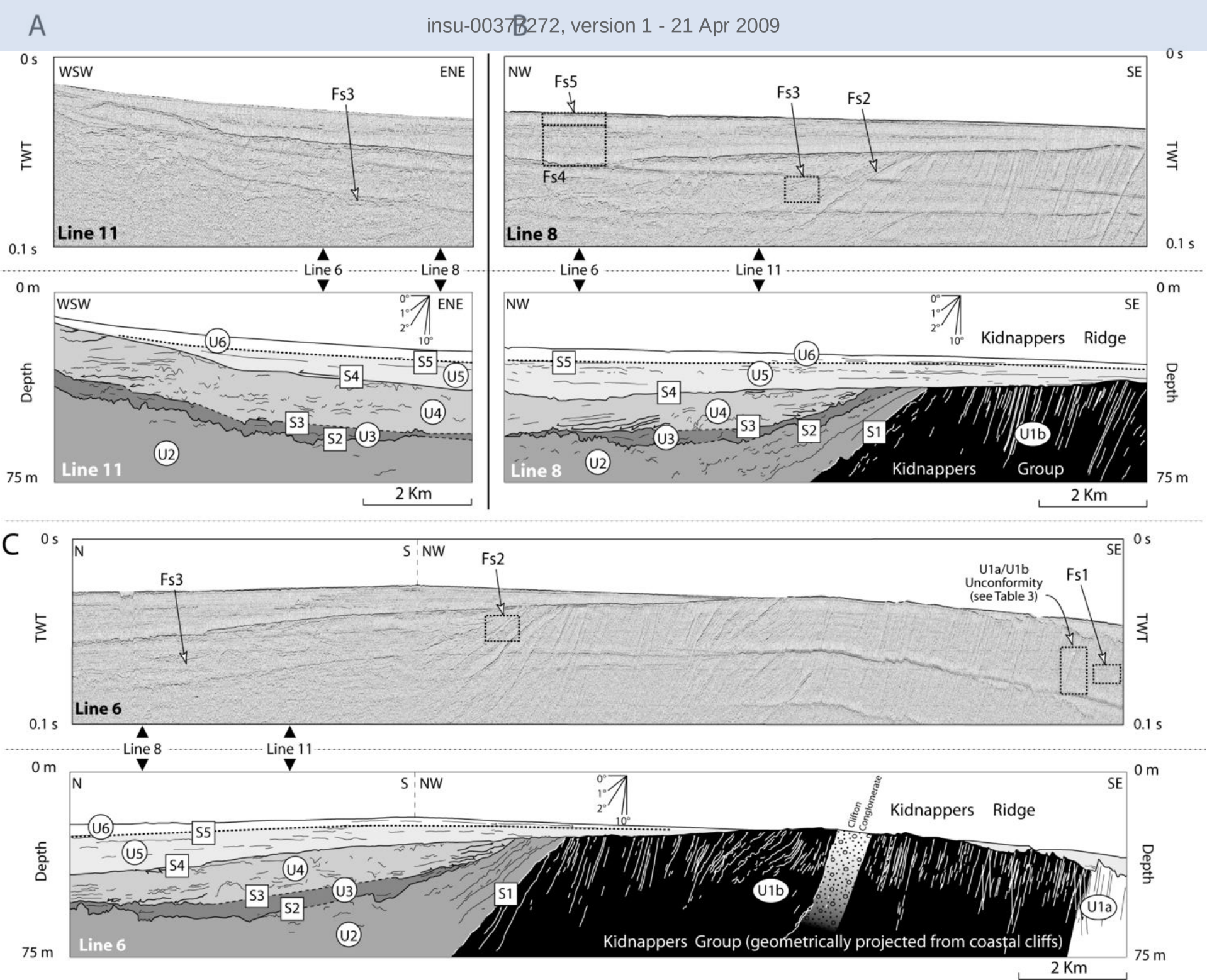
A
B
C
0 s
0.1 s
TWT
WSW
ENE
Fs3
Line 11
NW
SE
Fs5
Fs4
Fs2
Line 8
Line 6
Line 8
Line 11
0 m
75 m
Depth
U6
U5
U4
U3
U2
S5
S4
S3
S2
S1
0°
1°
2°
10°
Kidnappers Ridge
Kidnappers Group
2 Km
N
S
NW
Fs1
U1a/U1b
Unconformity
(see Table 3)
Clifton
Conglomerate
U1b
U1a
Kidnappers Group (geometrically projected from coastal cliffs)

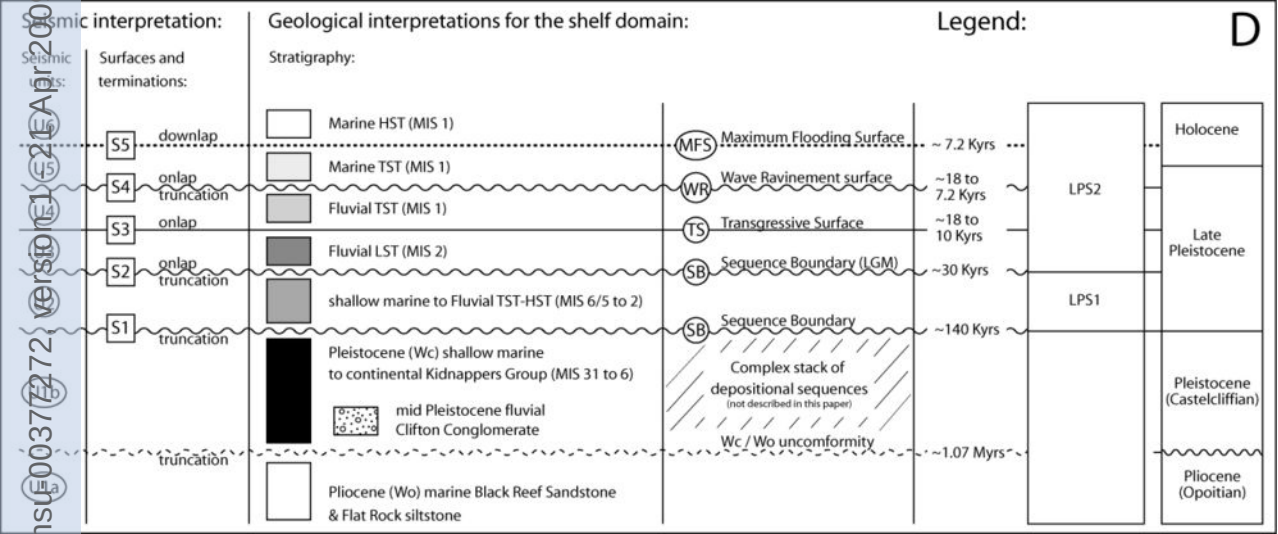
Seismic interpretation:
Geological interpretations for the shelf domain:
Legend:
D
Seismic units:
Surfaces and terminations:
Stratigraphy:
S5
downlap
S4
onlap
truncation
S3
onlap
S2
onlap
truncation
S1
truncation
truncation
Marine HST (MIS 1)
Marine TST (MIS 1)
Fluvial TST (MIS 1)
Fluvial LST (MIS 2)
shallow marine to Fluvial TST-HST (MIS 6/5 to 2)
Pleistocene (Wc) shallow marine to continental Kidnappers Group (MIS 31 to 6)
mid Pleistocene fluvial Clifton Conglomerate
Pliocene (Wo) marine Black Reef Sandstone & Flat Rock siltstone
MFS
Maximum Flooding Surface
~ 7.2 Kyrs
WR
Wave Ravinement surface
~18 to 7.2 Kyrs
TS
Transgressive Surface
~18 to 10 Kyrs
SB
Sequence Boundary (LGM)
~30 Kyrs
SB
Sequence Boundary
~140 Kyrs
Complex stack of depositional sequences
(not described in this paper)
Wc / Wo uncomformity
~1.07 Myrs
LPS2
LPS1
Holocene
Late Pleistocene
Pleistocene (Castelcliffian)
Pliocene (Opoitian)

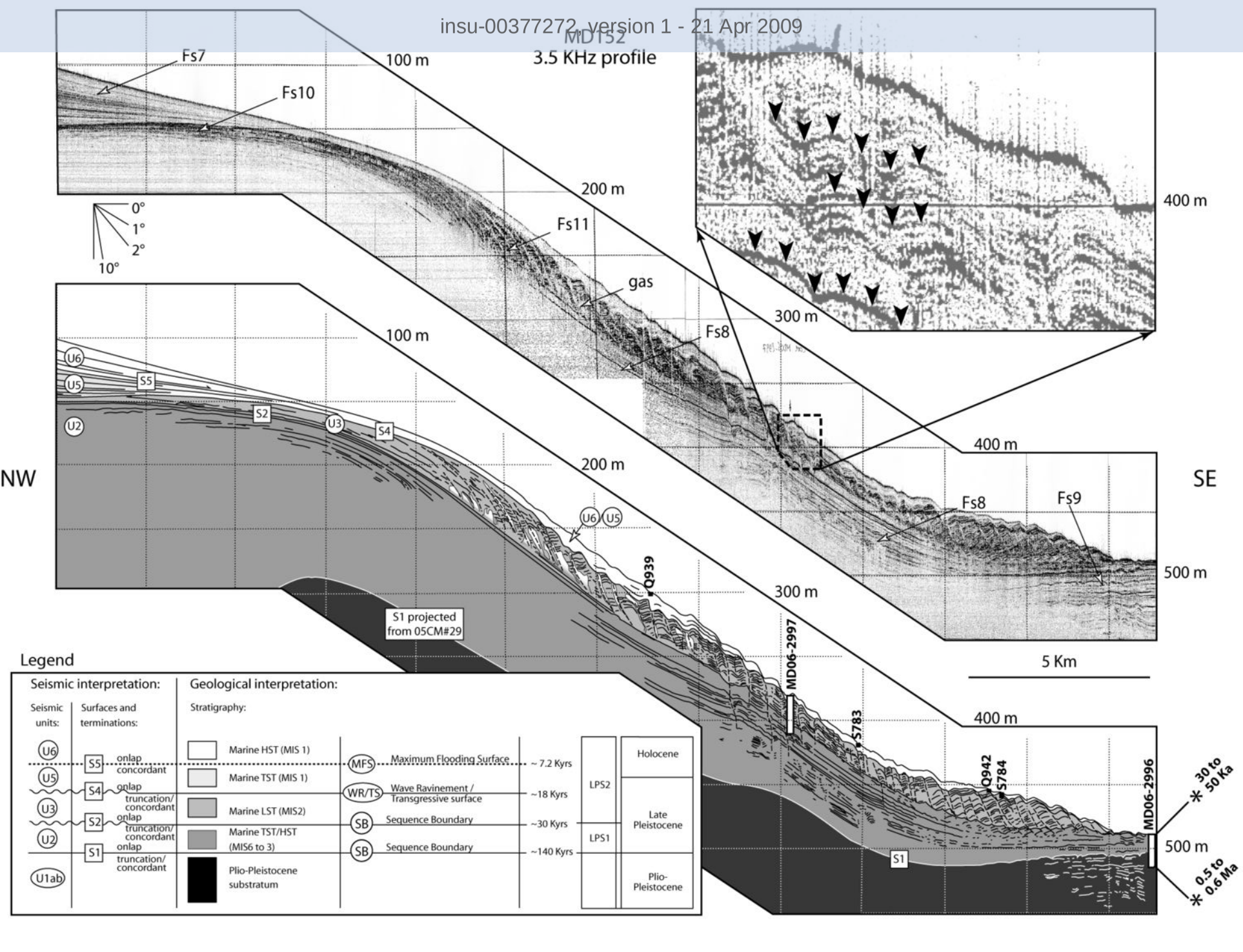

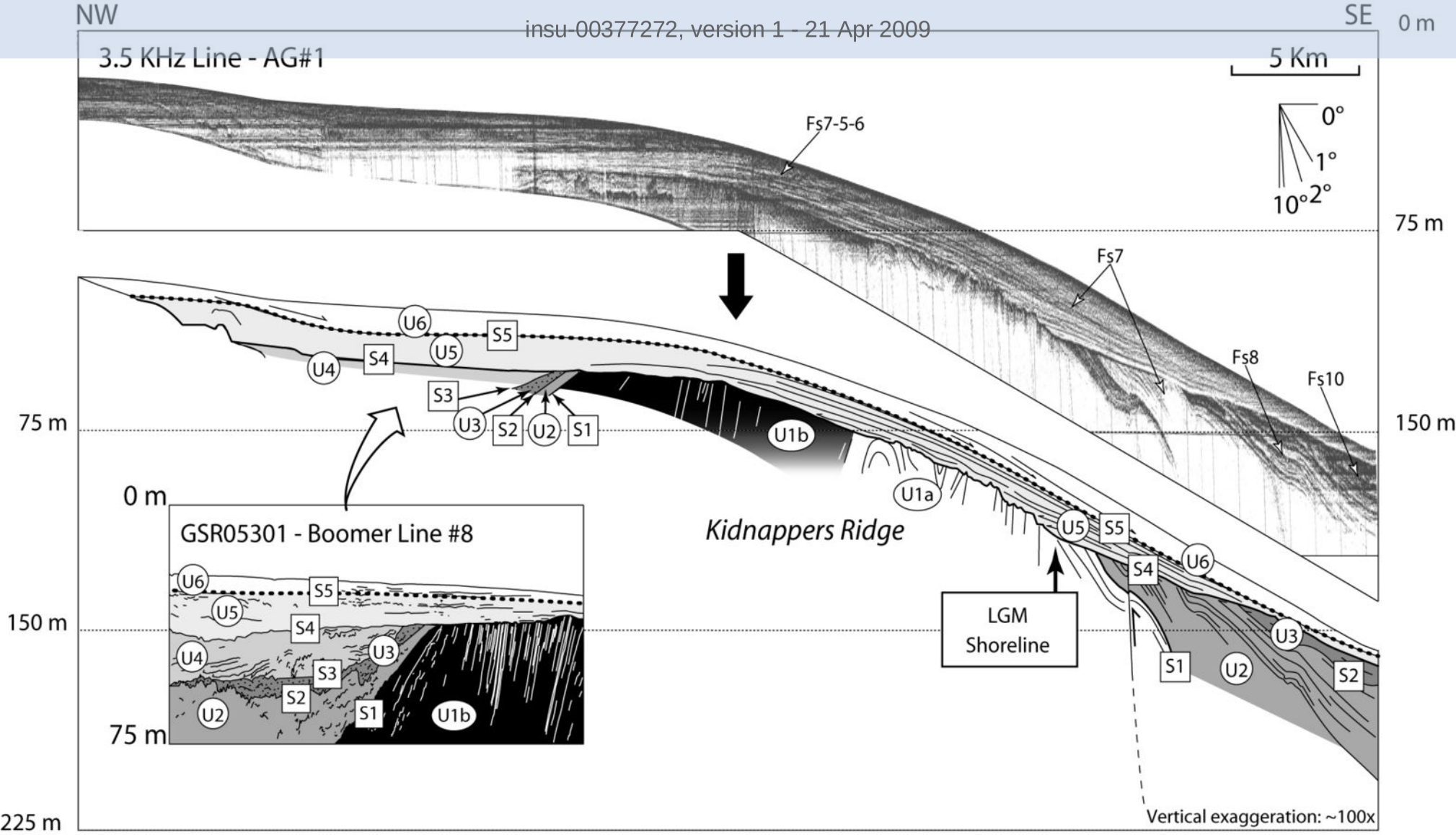

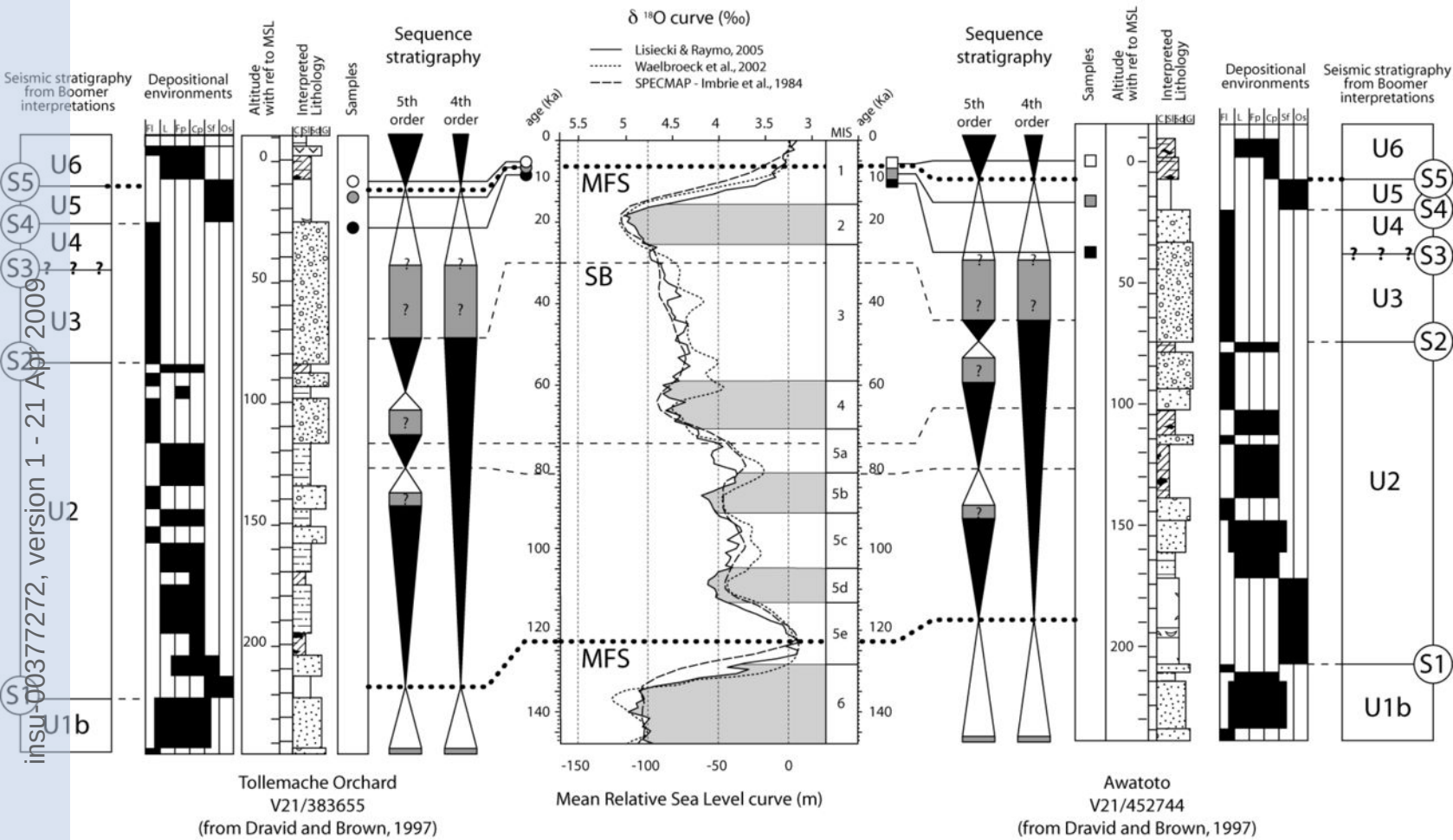

Abreviations use for depositional environments and grain size scale:

- Fl : Fluvial
- L : Lacustrine
- Fp : Flood plain
- Cp : Coastal plain
- Sf : Shoreface
- Os : Offshore sup
- C : Clay
- Sl : Silt
- Sd : Sand
- G : Gravel

Lithology (depositional environment):

- Gravel (Fluvial)
- Sandy gravel (Fluvial)
- Sand (Fluvial to shoreface)
- Sandy silt (Lacustrine to Coastal plain)
- Silty clay (Lacustrine to Coastal plain)
- Carbonaceous silt & clay (Flood plain to Coastal plain)
- Fossiliferous silt & clay (Shoreface to shallow marine)

Selected dated samples from Dravid & Brown (1997):

- Fossil Record V21/f215 - 5660 +/- 70 yrs BP (wood)
- Fossil Record V21/f246 - 8320 +/- 80 yrs BP (shells)
- Fossil Record V21/f273 - 10247 +/- 99 yrs BP (wood)
- Fossil Record V21/f117 - 5346 +/- 82 yrs BP (shells)
- Fossil Record V21/f123 - 6930 +/- 73 yrs BP (shells)
- Fossil Record V21/f132 - 7889 +/- 114 yrs BP (wood)

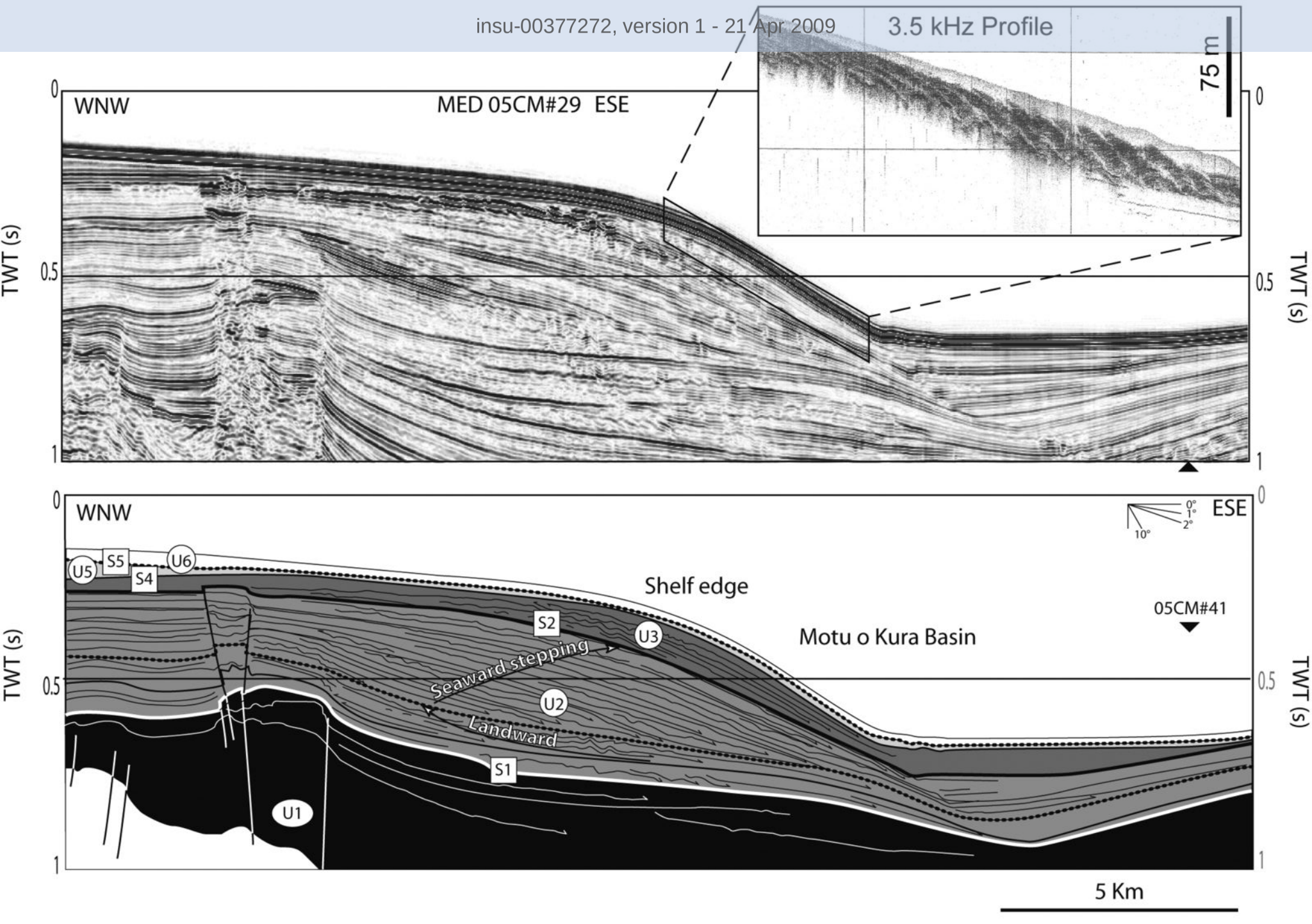

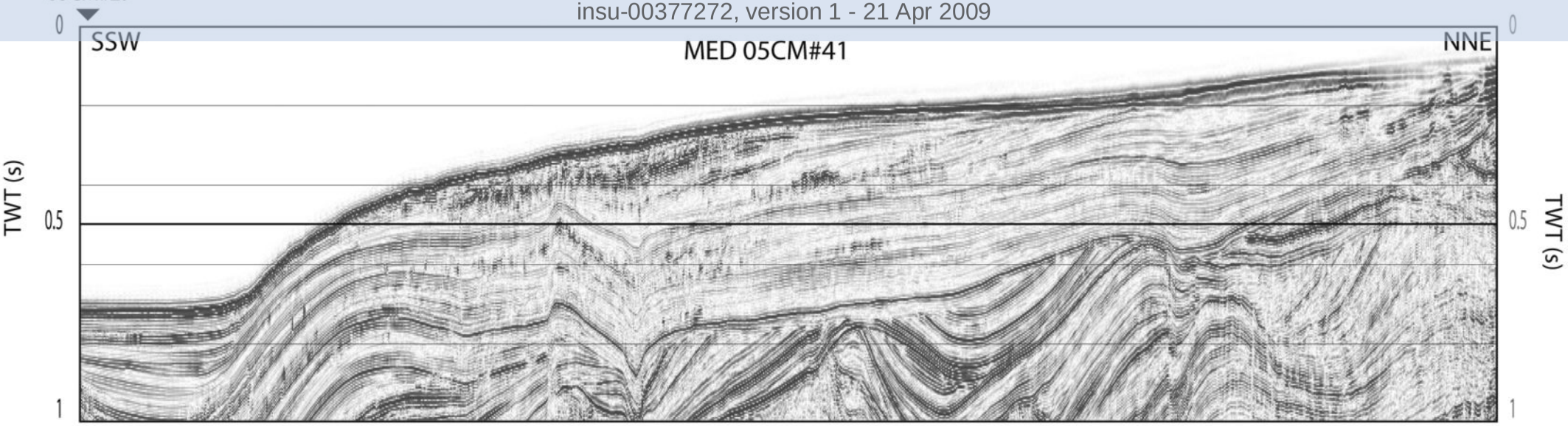
SSW
MED 05CM#41
NNE
TWT (s)
0
0.5
1

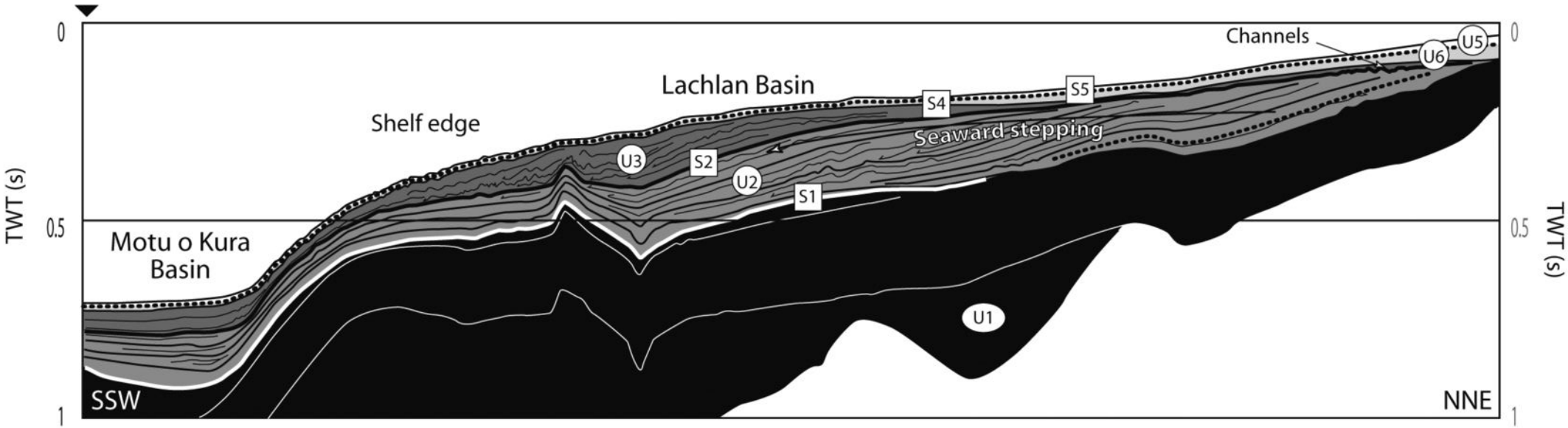
Channels
U6
U5
Lachlan Basin
S4
S5
Shelf edge
Seaward stepping
U3
S2
U2
S1
Motu o Kura
Basin
U1
SSW
NNE
TWT (s)
0
0.5
1

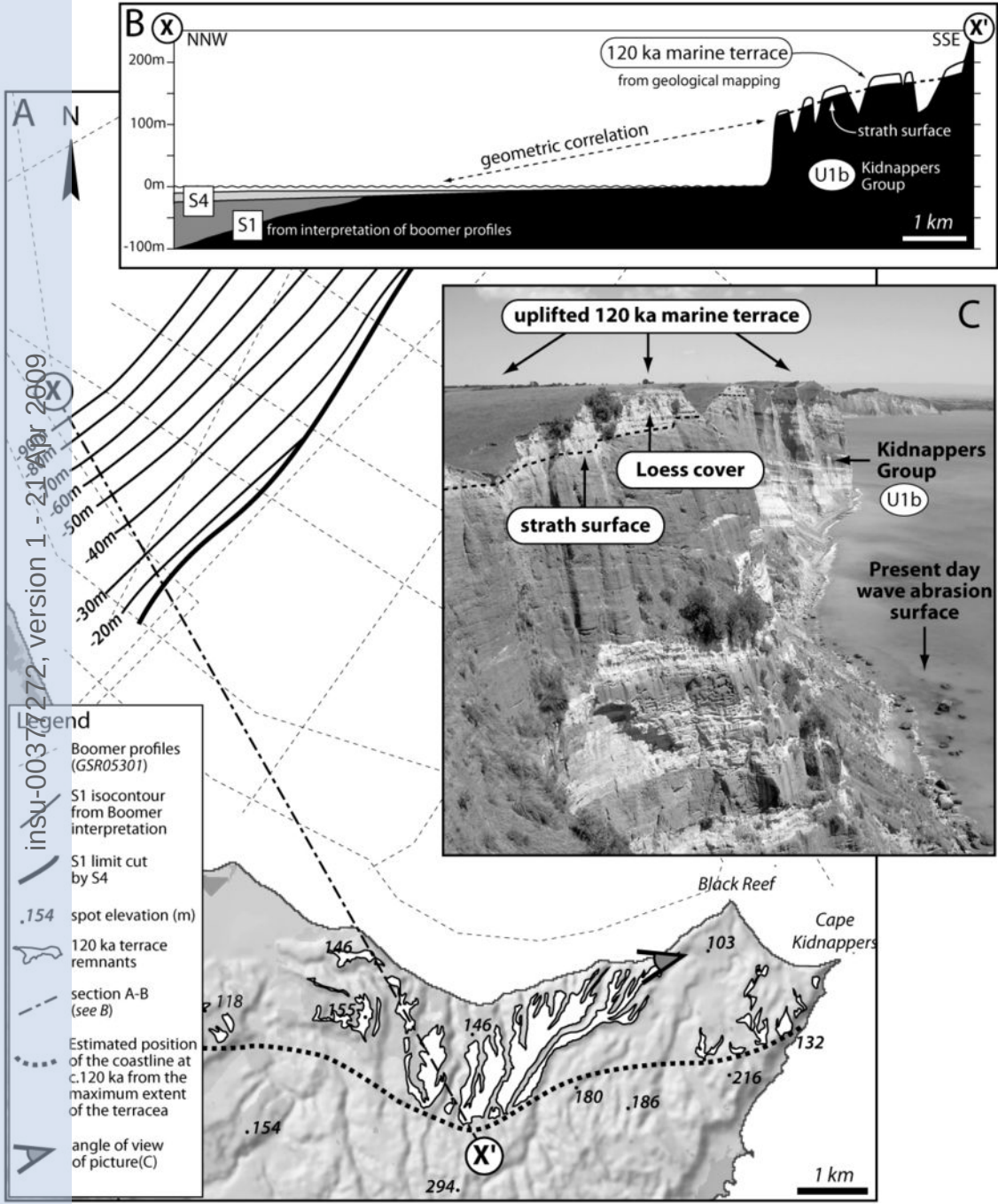

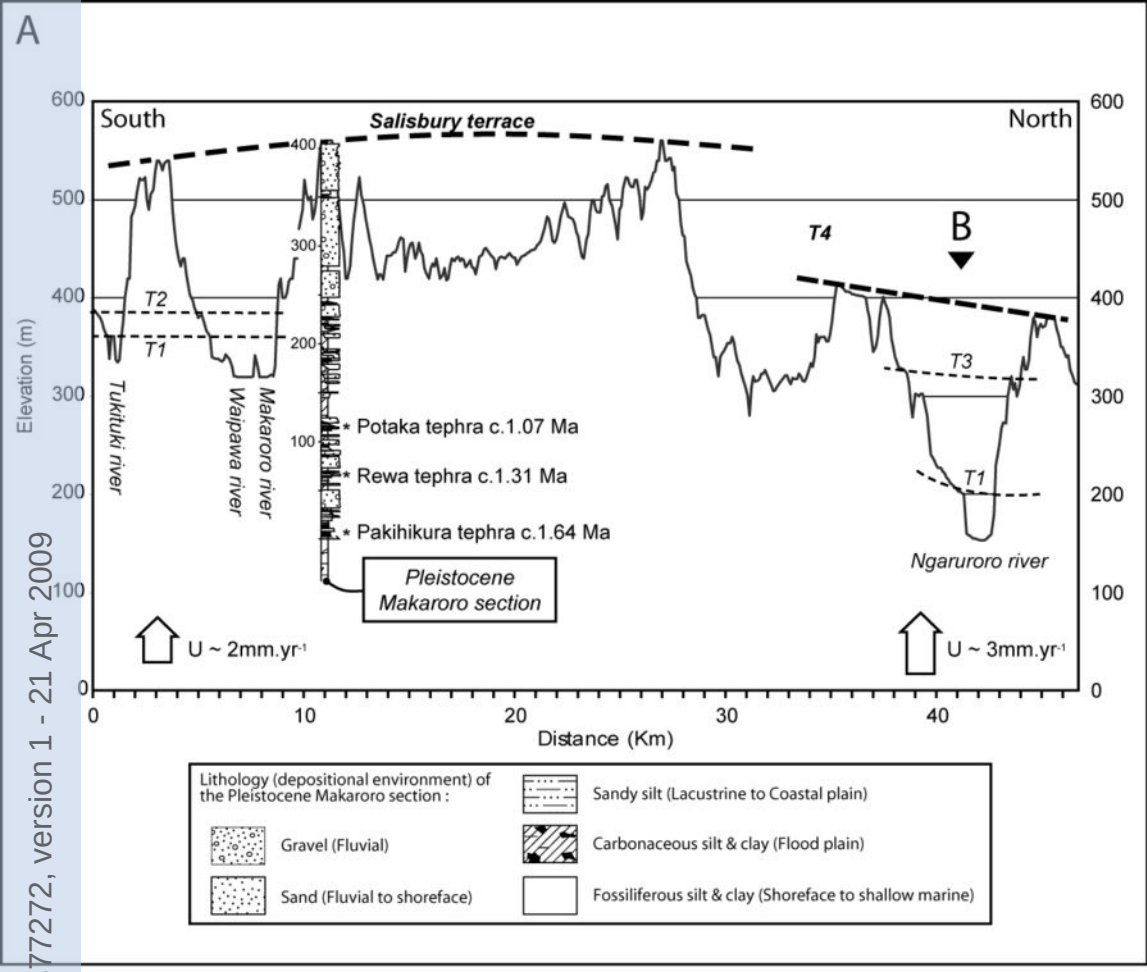

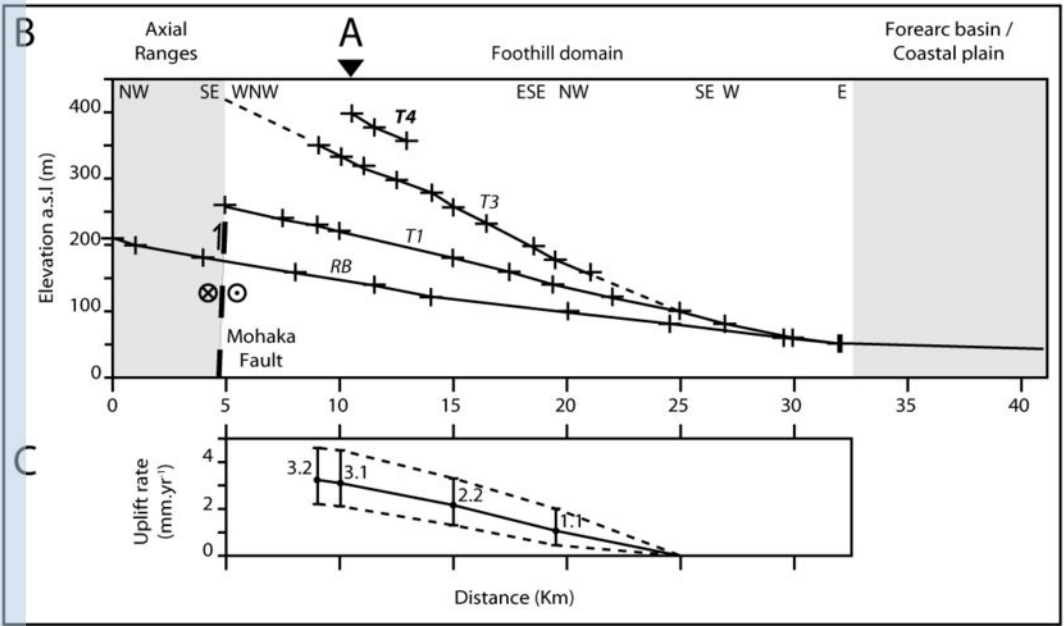

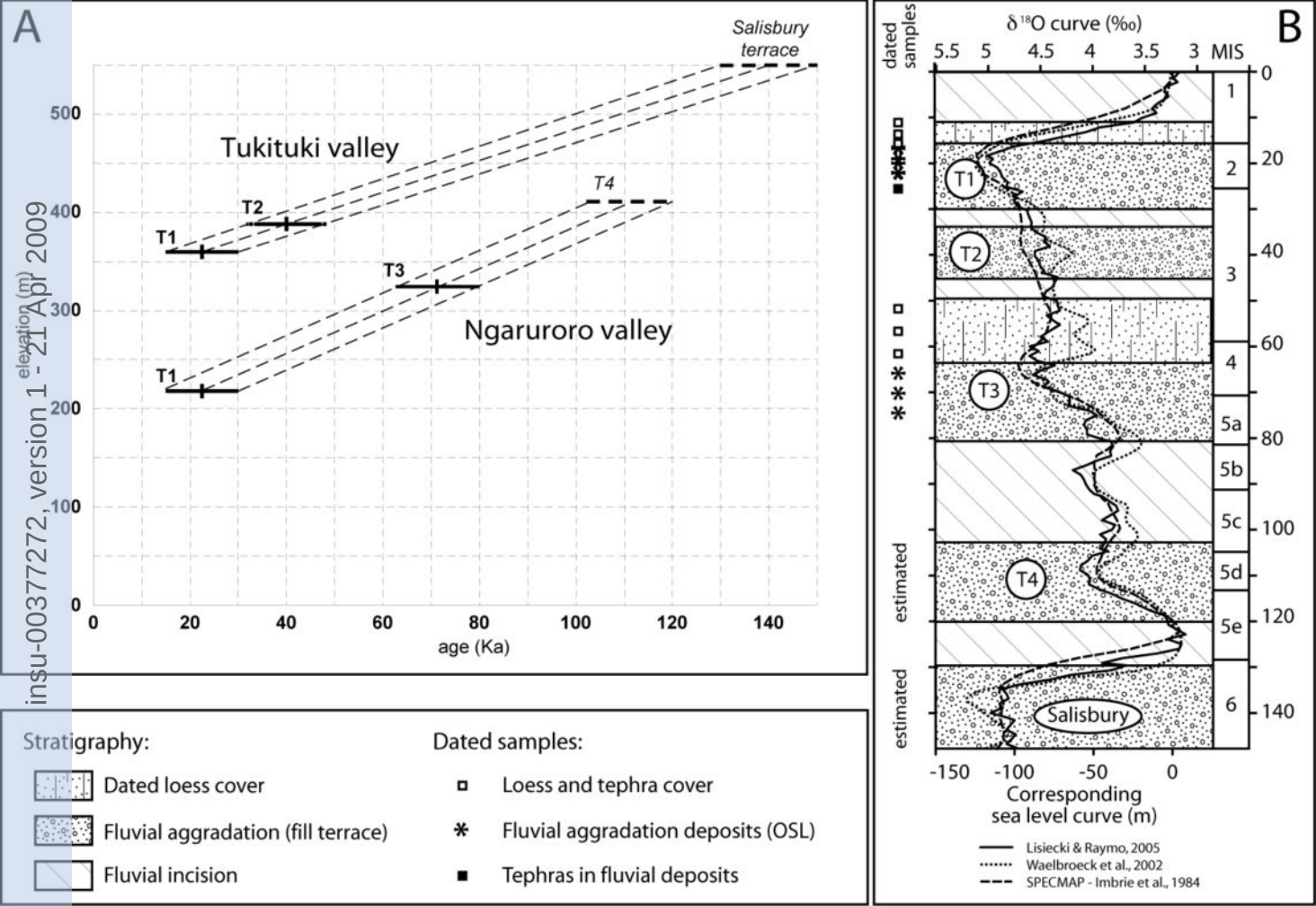

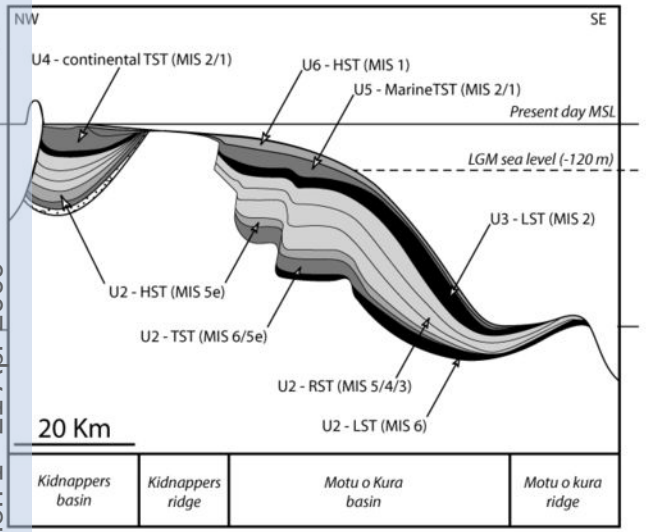

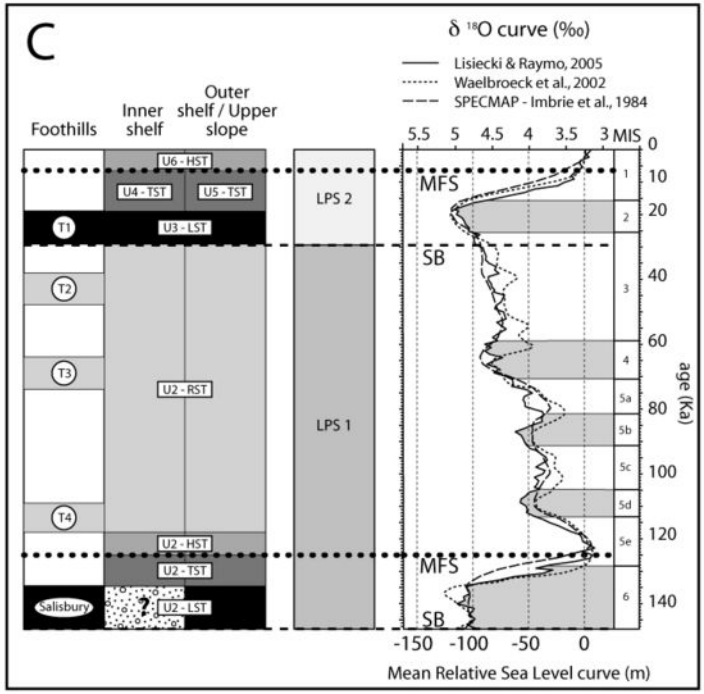

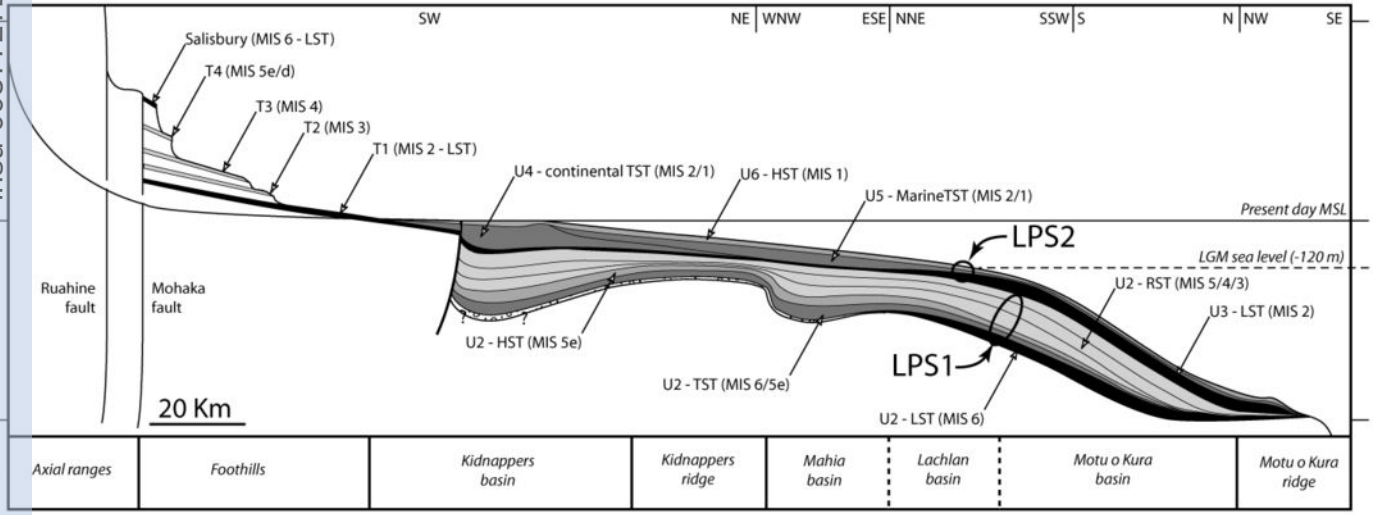

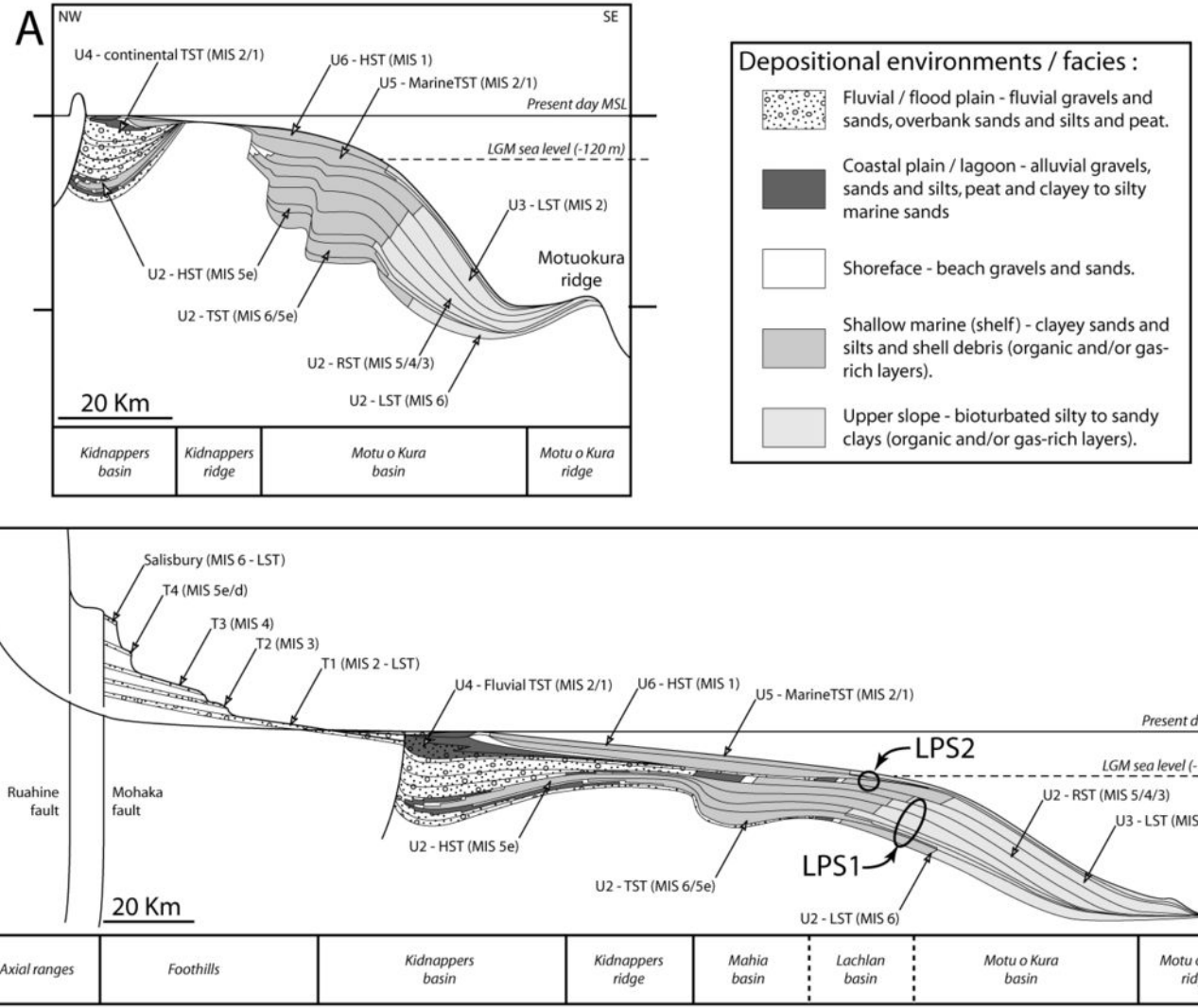

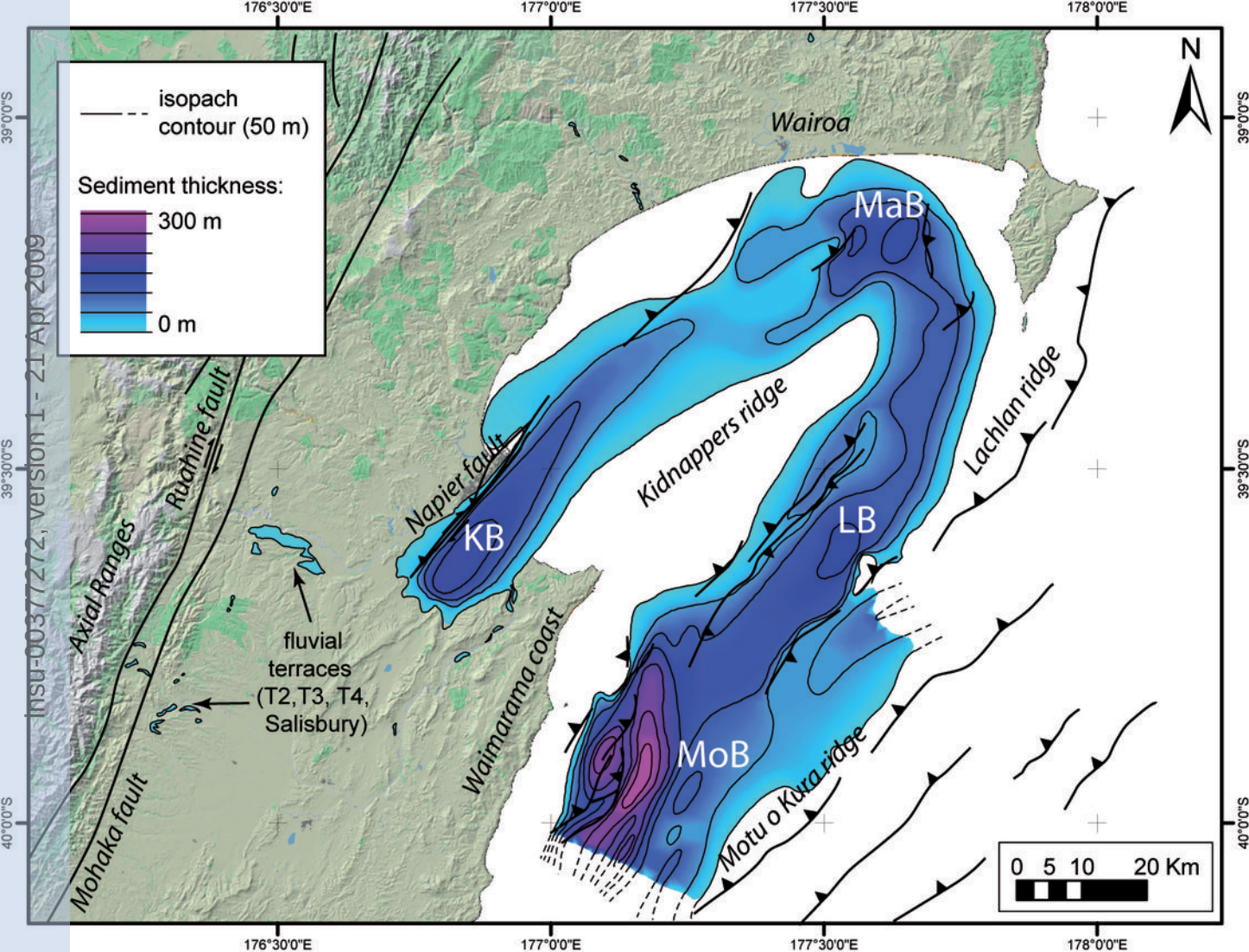

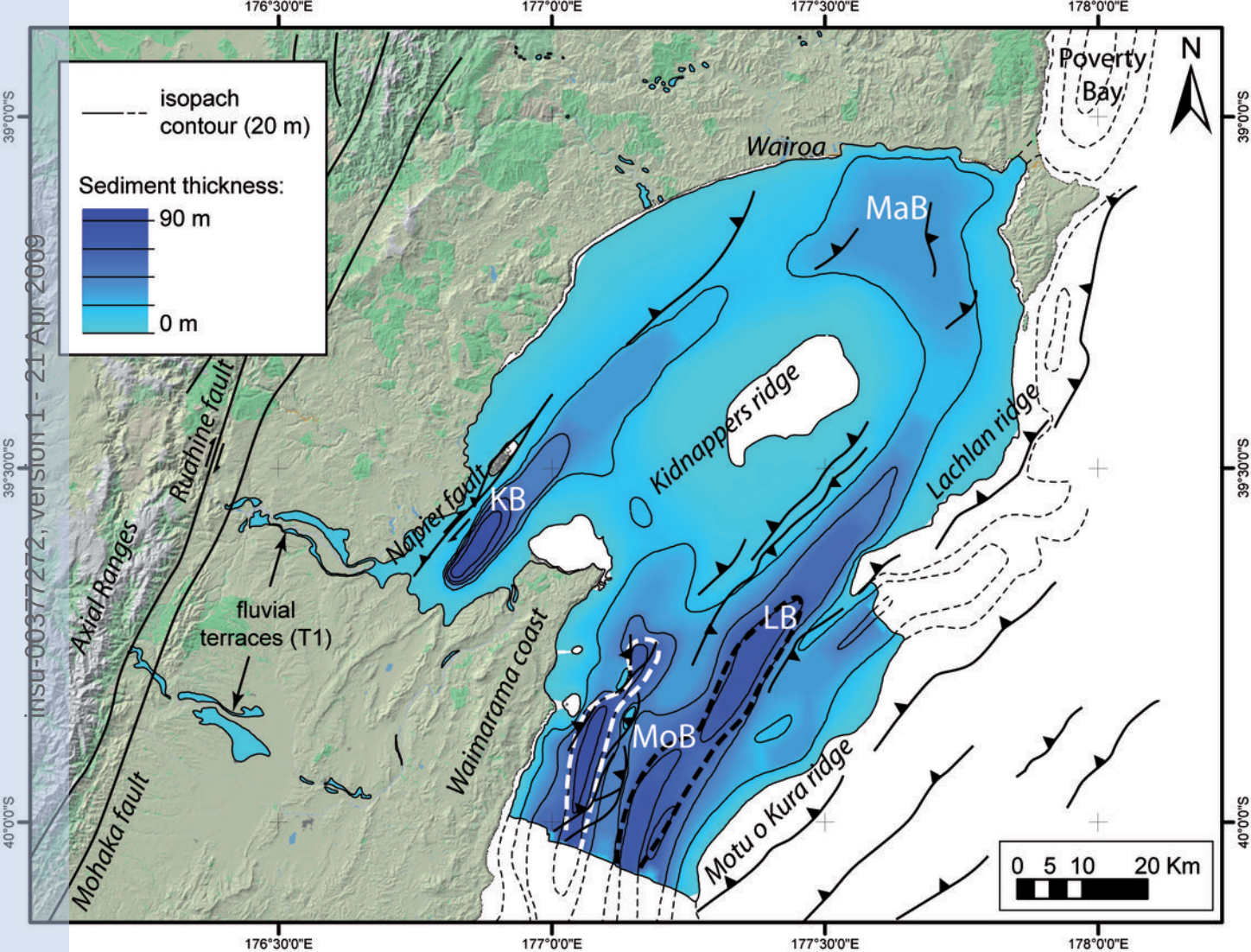

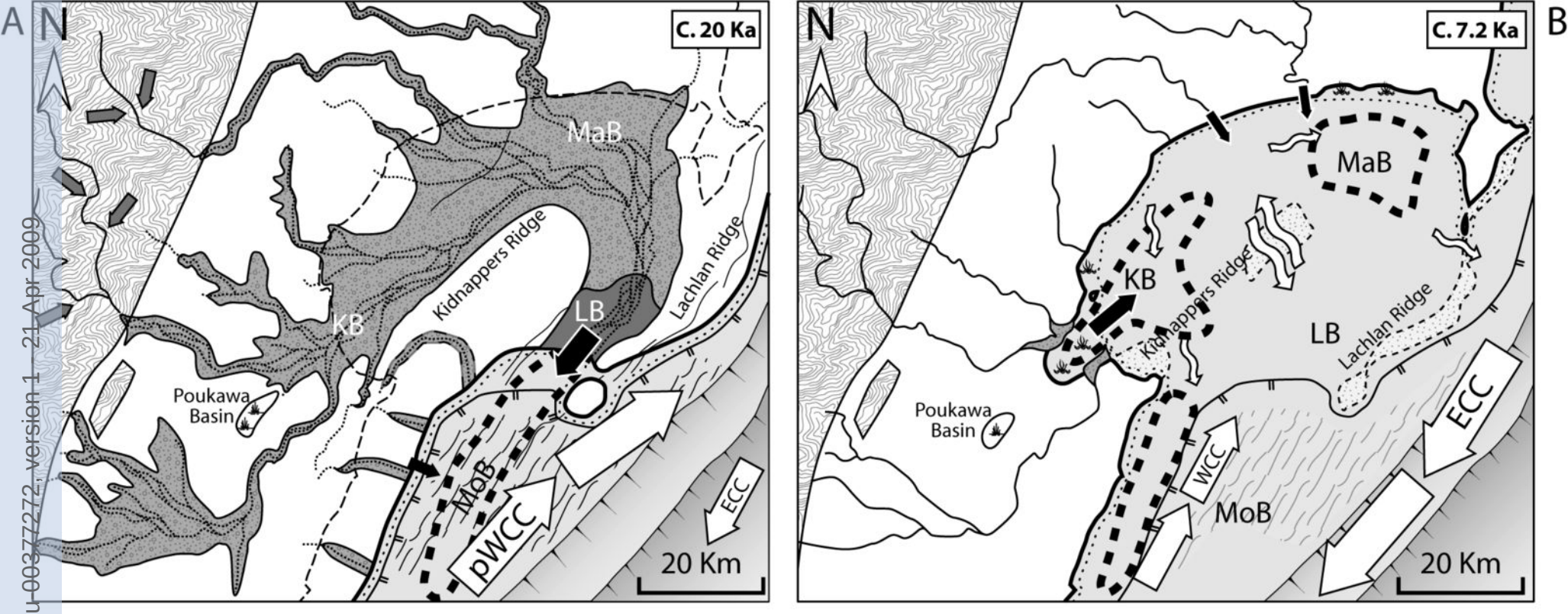

Table 1

Seismic units	Lower boundary surface	Upper boundary surface	Seismic facies
U1	-	S1, truncation	Fs1, Fs2, Fs3, Fs4, Fs5, Fs6
U2	S1, concordant	S2, truncation	Fs2, Fs7, Fs8, Fs9
U3	S2, concordant	S3, truncation	Fs3, Fs9, FS10, FS11
U4	S3, onlap	S4, concordant	Fs3
U5	S4, onlap	S5, truncation	Fs4, Fs7
U6	S5, onlap	seafloor	Fs5, Fs8

Seismic facies	Description	Interpretation	Examples	
			MCS	Boomer
Fs1	Good continuity, average amplitude, high frequency, parallel configuration	Well-bedded marine sandstones and siltstones	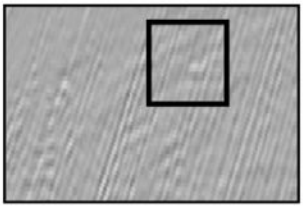	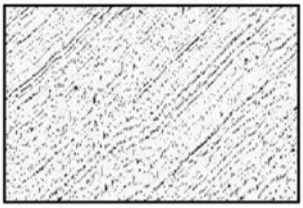
Fs2	Low to good continuity, low to high amplitude, average frequency, sub-parallel to chaotic configuration with channels	Shallow marine and terrestrial siltstones, sandstones, and conglmerates	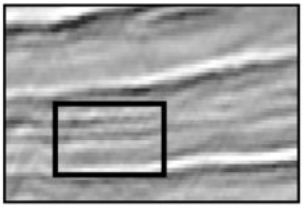	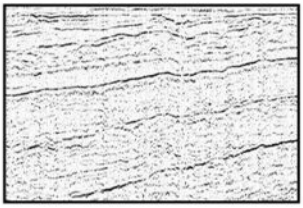
Fs3	Average to good continuity, low to high amplitude, average frequency, sub-parallel to chaotic configuration with incision channels	Fluvial gravels and overbank sand deposits	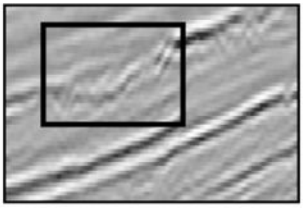	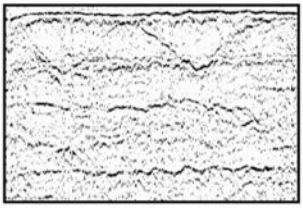
Fs4	Low to average continuity, low amplitude, average frequency, sub-parallel to chaotic configuration with small channels	Poorly-bedded shallow marine sand and silt succession deposited in a high energy shelf environment		
Fs5	Average continuity, transparent to low amplitude, low frequency, parallel to oblique parallel configuration	Poorly-bedded shallow marine sands and silts prograding towards the shelf break		
Fs6	Average to good continuity, low amplitude, high frequency, parallel configuration	Well-bedded shallow marine sandstones		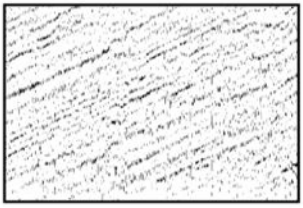

Seismic facies	Description	Interpretation	Examples	
			MCS	3.5 KHz
Fs7	Average to good continuity, low to average amplitude, low to average frequency, parallel to reflection free configuration	Shallow to deep marine sands and silts	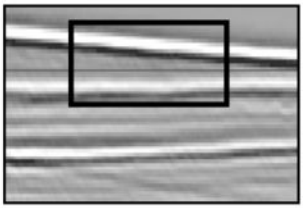	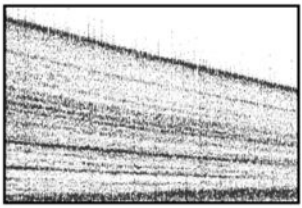
Fs8	Average to good continuity, average to high amplitude and frequency, parallel and slightly wavy configuration	Well-bedded deep marine silstones	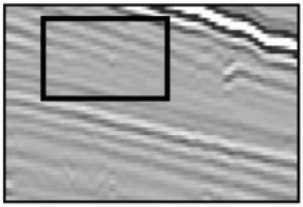	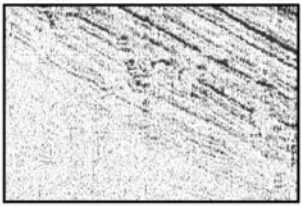
Fs9	Average to good continity, average to high amplitude and frequency, parallel and wavy configuration	Well-bedded and wavy deep marine siltstones	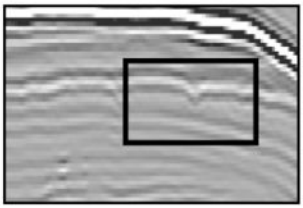	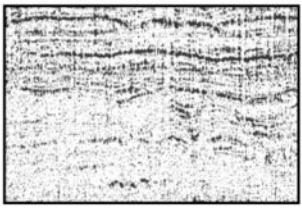
Fs10	Average continuity, high amplitude, average frequency, sub-parallel to chaotic configuration	Terrestrial to shallow marine sands with possible channels and gas	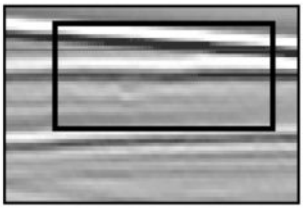	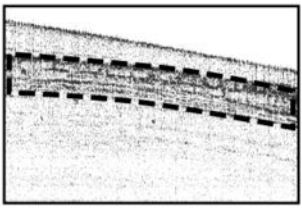
Fs11	Average to good continuity, high amplitude and frequency, undulating and parallel configura-	Well-bedded marine silty to sandy clays forming an extensive field of sediment waves	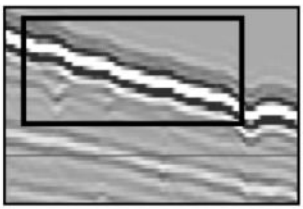	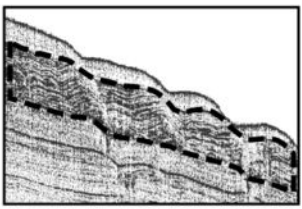
	Top lap / truncation surface separating U1a and U1b (see Fig. 5C)	Erosion surface at the base of the Pleistocene Kidnappers Group as observed onshore.		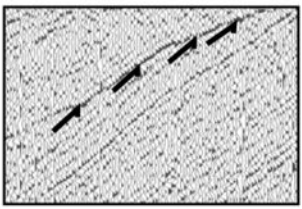

Appendix 1

Survey Name	Data type	Length (interpreted)	Operator / Country	Vessel	Year	Avaliable report (PR) or publications :
GeodyNZ	Bathymetry EM12		Ifremer / France	R/V Atalante	1993	Collot et al. (1996) Lewis et al. (1998)
Tan0106	Bathymetry EM300		NIWA / NZ	R/V Tangaroa	2001	
GSR 05301	Boomer	175 km	NIWA / CNRS	Big Kahuna	2005	
CQX H90	MCS (60 folds)	1000 km	NZ CQX Ltd.	M/V Western Pacific	1990	Sullivan – PR 1666 (1990)
05CM	MCS (640/960 channels)	720 km	Ministry of Economic Development / NZ	M/V Pacific Titan	2005	Multiwave – PR 3186 (2005)
CR3044	3.5 KHz & MCS (24 channels)		NIWA / NZ	R/V Tangaroa	1998	Barnes et al. (2002) ; Barnes and Nicol (2004)
TAN 0313	3.5 KHz & MCS (48 channels)	830 km	NIWA / NZ	R/V Tangaroa	2003	

TAN 0412	3.5 KHz & MCS (48 channels)	298 km	NIWA / NZ	R/V Tangaroa	2004	
CR8024	3.5 KHz	1200 km	Conquest Exploration Ltd / NZ	GRV Rapuhia	1988	Conquest Exploration - PR2059 (1988)
MD152 / Matacore	3.5 KHz & 6 giant calypso piston cores (MD06-2995/96/97 on the upper slope and MD06-2998/99 /3000 on the shelf)	c. 100 km (core length up to c. 30 m)	IPEV / CNRS-INSU / NIWA / AWI / VIMS SIO	R/V Marion-Dufresne	2006	Proust et al. (2006)